K O N I N K L I J K N E D E R L A N D S
M E T E O R O L O G I S C H I N S T I T U U T

D e B i l t

WETENSCHAPPELIJK RAPPORT

W.R. 76-5

H.M. de Jong

Study on the system mix of radiosonde aircraft and satellite observations in the North Atlantic region

Observational characteristics and data processing

De Bilt, 1976.

Publikatienummer: K.N.M.I. W.R. 76-5 (MO)

U.D.C.: 551.501.4 :
551.509.1 :
551.547.5 :
551.507.352

ABSTRACT

In oceanic regions there are three upper air observation systems in operation now: the space-based satellite radiance system (NOAA series) and the surface-based radiosonde/rawin and aircraft reporting systems. These various data sources constitute what is called a "system mix".

First the observational techniques and programmes are reviewed with a special emphasis on the observational characteristics of the various systems individually and in combination. These observational characteristics are discussed within the framework of the observational data requirements as established in the WWW-plan.

Special attention is paid to the monitoring of the performance of the air reporting system.

The data conveyed by the system mix need a form of preprocessing before they are suited to be used in the preparation of upper air charts or inserted in numerical weather prediction models.

The paper deals with the main aspects of this data processing. It describes in particular a method to derive the absolute geopotential height in aircraft locations from all available data in the system mix. Use is made of a special geopotential theorem. The evaluation of this theorem requires the introduction of some graph theoretical concepts in the network of available data points.

The processed data, when subjected to an additional selection procedure and interpolation to the nearest standard pressure levels (300, 250 and 200 mbar), together with updated satellite data clearly contribute to a better definition of the physical state of the atmosphere.

One section is devoted to the important problem of quality control of the received data. The solution proposed here is

based on a special triangulation check within an appropriate geometric graph structure.

The report concludes with a discussion of the processing of very detailed meteorological information retrieved from the records submitted by aircraft equipped with automatic data acquisition units.

-o-o-o-

TABLE OF CONTENTS

INTRODUCTION

In meteorology the definition of the state of the atmosphere requires the provision of sufficient and accurate information on the state variables on a regional and global scale.

This information is to be retrieved from observations which are submitted by various surface-based and space-based observational systems.

In the planning and implementation of the Global Observing System it is the purpose to coördinate all methods, techniques and facilities for making the observations in a rational way.

Part of the observational material can be supplied by the various independently functioning observation systems and may directly be used as basic data for further manual or numerical analysis and prediction. Other data need to be subjected to some form of pre-analysis processing before they are suited to be inserted in numerical models.

In case of a blend of data coverage in space and time in a mix of observation systems the available data sets may serve as primary data to derive or update valuable additional upper air data. This presupposes the availability of some efficacious diagnostic tools and suitable algorithms to be used in the processing of observations conveyed by the components in a system mix.

The increasing use of data submitted by the components in a system mix also requires the evaluation of data accuracies, representativeness and compatibilities. In a system mix there is also the problem of how to find a well-balanced observational programme. To arrange for an appropriate minimum observational programme we need some adequate means to specify the performance characteristics of each component system separately.

But in practice such a specification can meet with difficulties because of operational and technical limitations. It is difficult for example to modify existing standards and practices of air reporting procedures, mainly due to restrictions imposed by Air Traffic Control.

The present study is devoted to an analysis of the system mix of three upper air observation systems in the North Atlantic Region in terms of data requirements and pre-analysis processing. The mix of observation systems consists of the conventional WWW-network of radiosonde/radar observations, the aircraft meteorological observations and the satellite radiance observations.

In part I a review is given of the present observational techniques and programmes of each separate component system. Special attention is paid to the problem to what degree the observational data requirements are fulfilled as established in the WWW-plan. (See Annex to this report). From that some inferences are drawn with respect to the specification of the data requirements in the mix of observation systems.

The problem is of fundamental importance from a point of view of the planning of WWW. One of the principles of WWW-implementation is that no component or facility should be removed before studies have demonstrated that the corresponding new component or facility can meet the requirements at least to the extent of the old.

Part II deals mainly with the problem of pre-analysis processing in the above-mentioned system mix over the Atlantic. A new method is proposed to pre-process all available data which can be retrieved from the reports of these observations (TEMP/PILOT, AIREP, SIRS). This method of "combined processing" in a system mix is centred about an application of a powerful diagnostic expression in the form of a line integral. This expression is deducible from the well-known hydrostatic equation and the geostrophic wind approximation. The expression is also suitable to be used for quality control purposes. The feasibility of the method is demonstrated by some computer experiments.

-o-o-o-

P A R T I

1. The mix of upper air observation systems in the North Atlantic Region

Part I introduces the various aspects of the observational techniques and programmes involved in the system mix of upper air observations in the North Atlantic Region. This is done primarily by consideration of the characteristics and features of each sub-system within the framework of the established observational data requirements. The examination of the various attributes in each sub-system is of fundamental importance in connection with the problems of the specification of the data requirements and combined processing in the system mix.

Later on, in Part II, we will observe that in the scheme of combined pre-analysis processing the data handling of aircraft meteorological observations plays a prominent part. This explains why in this section much attention is paid to the performance aspects of the air reporting system.

1.1 Review of observational techniques and programmes

1.1.1 Radiosonde/rawin observations

The conventional WWW upper air observing system continues to be the main source of information required to meet regional and national requirements especially over land areas. In the system mix under consideration over the North Atlantic the WWW-network consists of the near-shore stations, some island stations and of some stationary ships (NAOS-network).

From a point of view of combined pre-analysis processing the NAOS-network will appear to be extremely important. The NAOS-network came into existence in 1948 under the auspices of ICAO. It had as its primary purpose the provision of meteorological data to assist to the safe, regular and economic operations of airline services. The importance of the NAOS-network to aviation has diminished to some extent, whereas its importance to meteorology within the framework of WWW has greatly increased. It was recognized

that although a reduction of the scheme was inevitable, any continuing requirement for the NAOS-network should be within the framework of WMO rather than of ICAO. A new agreement was developed under the auspices of WMO. At the time of writing this study the agreement had not come formally into force yet, but was applied provisionally. The network consists of four stations. The details of the radiosonde/rawin observation system are well known and need not be discussed further.

1.1.2 Aircraft meteorological observations

The WWW-programme may have access to sources of information of other international programmes. In the relationship between WMO amd ICAO the air reporting system is such a source of valuable meteorological observations.

The standards and practices of air reporting are laid down in WMO and ICAO regulatory documents [1,2,3]. An air report is prepared in the course of the flight, in conformity with requirements for position, operational or meteorological reporting in the AIREP-form. The meteorological information is contained in section 3 of the report. Items which need to be reported to provide a suitable meteorological data set comprise aircraft identification, position, time, flight level or altitude, air temperature and spot- or mean wind. The reports are transmitted directly to ATC-centres and relayed for onward transmission including the GTS, in accordance with ICAO and WMO procedures. In the NAT-region not all meteorological information available is transmitted directly air-to-ground in view of some regional exemption procedures. This information is not lost, however, as on arrival of a flight at an aerodrome the records of meteorological observations (flight meteorological log) are delivered by the operator without delay to the meteorological office.

These series of post-flight reports contained in the flight meteorological logs may constitute another source of valuable meteorological data.

Wide-bodied aircraft (DC-10, Boeing 747) now become equipped with automatic data acquisition units, which under control of an airborne computer make records of a vast amount of flight data including meteorological parameters. Registration can be performed every 600 milliseconds, although at present recordings are made every 400 s, except during ascent and descent. When recording is continuous this technique adds a new dimension to the supply of highly detailed meteorological data. Full utilization of these data on a routine basis may need the development of new transmission techniques using high speed data links or satellites.

The observational programme is closely related to the organization of the air traffic. The overall traffic is governed by the companies' traffic patterns and time schedules.

In the NAT-region the traffic is mainly split up in an eastbound and a westbound stream. These traffic flows are separated in time. The peak hour in the eastbound traffic flow is around 0400 GMT, in the westbound traffic flow around 1600 GMT. Often both traffic flows are also separated in space. This is related to the principle of optimal track selection in the prevailing atmospheric circulation. Statistically, in the organized track system the westbound traffic appears to be also northbound, and the eastbound traffic also southbound. In the vertical the traffic is furthermore concentrated within a narrow corridor, roughly between 300 and 200 mbar. As a consequence, the routine meteorological reports cover only a limited airspace. The frequency and location of the reports are related to the ATS reporting procedures. Routine reports are made at one-degree latitude points on successive 10-degree meridians. This causes a clustering of reports along the reporting meridians with great hiatuses in between.

In the continental airway zones some additional reports are made the locations of which are either identified by name or in relation to a significant geographical feature or by identification of the navigational aid at the reporting point.

At cruising altitude the vertical coördinate is defined by the flight level number expressed in units of 1000 ft. The present criteria for vertical separation make that in both the eastbound and westbound traffic the reports apply to uneven flight level numbers (Fl 29, 31, 33, ..). When the system of composite separation is applied, then the reports refer to even flight level numbers.

Taking the criteria for vertical, lateral and longitudinal separation into account, the occurrence of multiple space-time observations is precluded.

An implication of the ATS reporting procedures is that the network of aircraft observations is a fixed 3-dimensional network, but the occupation of network points with data is variable in time and space.

From a point of view of data processing it is important to investigate the data supply in more detail. To obtain an impression of the data supply a few counts have been made of air reports received over the GTS in a 24-hour period at hourly intervals in De Bilt (06260) on 5-01-75. Fig. 1 shows a histogram of hourly collectives of reports as a function of the hour of the day. Fig. 2 shows the same type of histogram valid for each reporting meridian 10^{o}, 15^{o}, 20^{o}, 30^{o}, 40^{o} and 50^{o} W. Fig. 3, in the form of a table, shows the distribution of reports per flight level as a function of the hour of the day. Eliminated from the counts were the many duplicates of messages received. The data supply is directly coupled with the structure of the air traffic, so that the statistics allow the following interpretation. In the NAT-region the observational programme of the air reporting system provides for a continuous supply of meteorological data. Associated with the eastbound traffic the data flow progresses like waves from west to east. Coupled with the westbound traffic the data flow progresses from east to west. At each reporting meridian the data supply is recurrent with a periodicity dependent on the longitude.

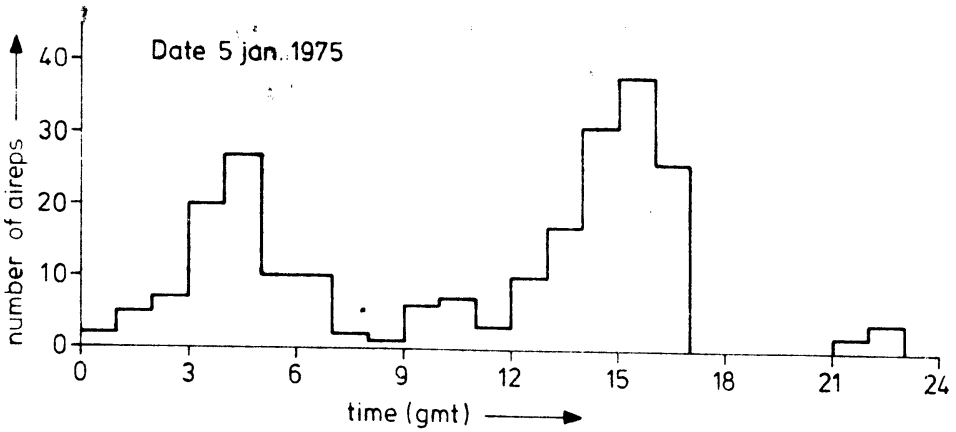

Figure 1 Distribution of aircraft reports as received on 5 January 1975 at De Bilt.

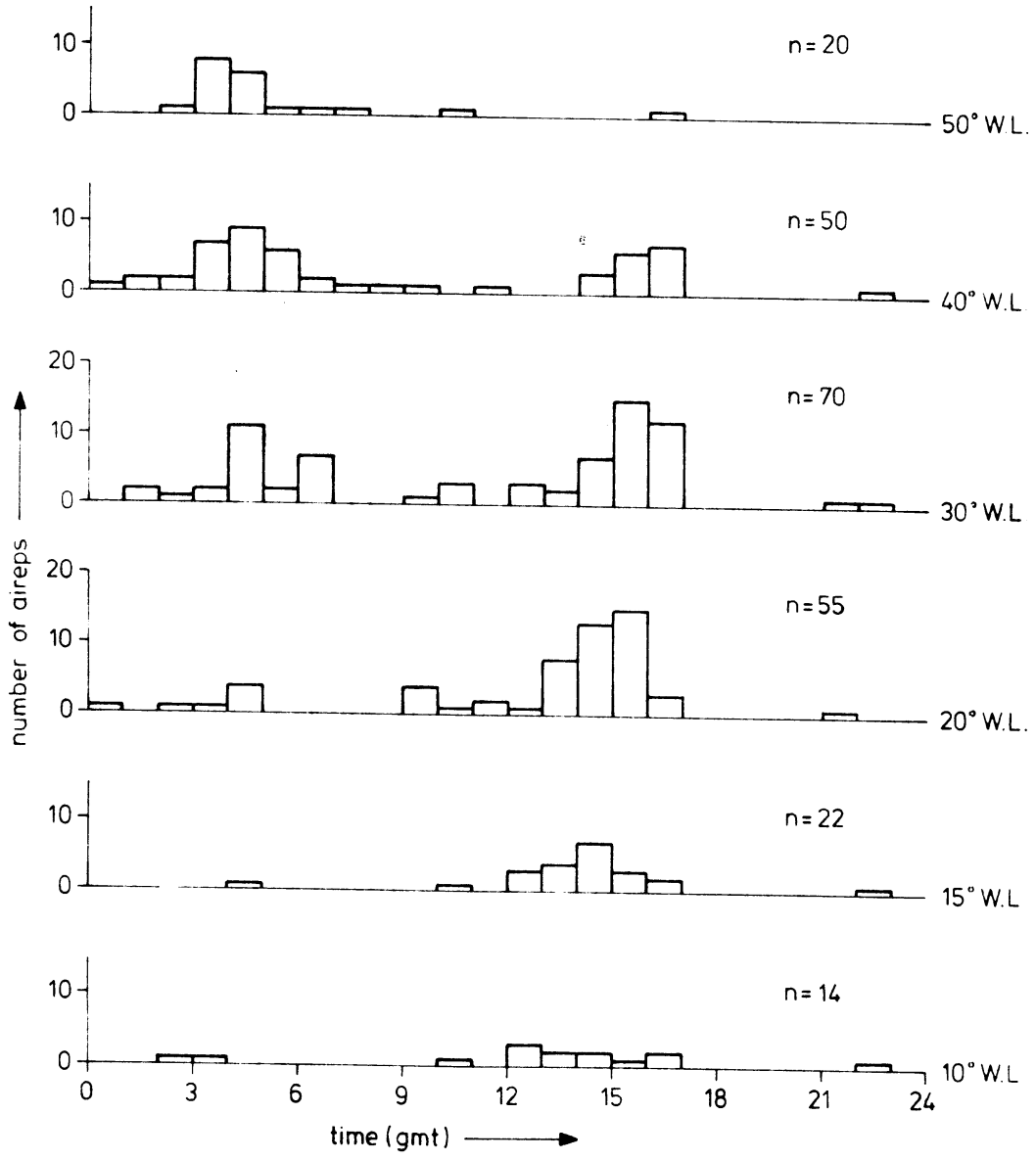

Figure 2 Distribution of aircraft reports as received on 5 January 1975 at De Bilt, per reporting meridian.

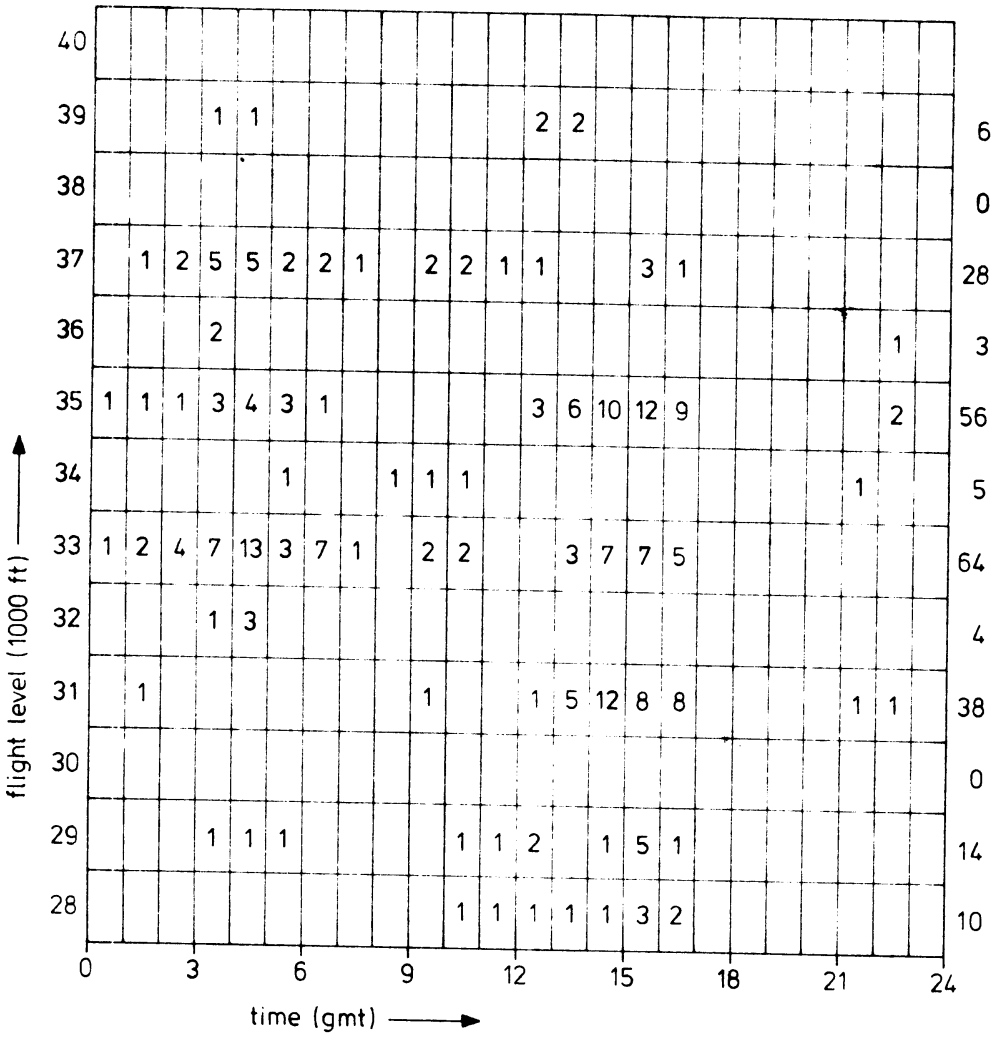

Figure 3 Distribution of aircraft reports as received on 5 January 1975, per flight level.

From Fig. 1 we may infer that the data supply shows a periodicity of approximately 12 hours with peak supplies 3 to 4 hours off-standard times. When charts are prepared valid at the main synoptic hours this means that a cut-off time of several hours is required to collect a sufficient number of mid-oceanic aircraft reports. Around 00 GMT the density of data points is highest in the western part of the Atlantic, around 12 GMT highest in the eastern part.

Fig. 3 indicates that the highest occupation of data is with the uneven flight levels, as expected. An important feature of the data processing to be described in Part II is the selection of flight levels relative to the nearest standard pressure levels 300, 250 and 200 mbar. These levels correspond to a pressure altitude of 30065, 33999 and 38662 ft. When the air reports are sorted in terms of these nearest pressure levels, the majority of the reports will be related to the 250 mbar level.

Another point of interest is to have an impression of the performance of the air reporting system in the NAT-region.

The number of transatlantic crossings in winter amounts to approximately 200 per day. Assuming that in the 10^{o} reporting system each flight makes at least 5 reports, it may be concluded that there is a daily potential of about 1000 mid-oceanic reports. A great number of these reports is not distributed during the flight, because in the NAT-region not all aircraft are obliged to transmit the reports. Only flights participating in the organized track system and cleared by the phrase "SEND MET REPORTS" do transmit the reports directly air-to-ground.

From the material used to deduce the above statistics we could infer that the reports were produced by merely 90 flights. This reduces the volume of available in-flight reports to approximately 500. The amount of reports actually received was about 200. These were distributed over the flights as follows:

number of reports per flight	number of flights
1	27
2	25
3	23
4	10
5	5

Thus on the average slightly more than 2 in-flight reports per flight actually reach destination, so that for some unknown reasons more than 50% of the reports available is lost.

It is recognized that a reduction on this scale causes a considerable loss of valuable basic meteorological information. Meteorological centres which use conventional methods in the preparation of charts do not consider this reduction as a serious drawback, as the volume of AIREPs received is already scarcely manageable. Centres equipped with powerful computers, which can process large quantities of basic data in an almost negligible time, will however welcome any improvement in the distribution of these basic data. The surplus of data not only improves the data resolution and representativeness, but also aids in the quality control of the reports by redundancy.

The structure of the information flow of AIREPs is typical for the North Atlantic Region. A similar study has revealed that in the western Pacific the information flow is characterized by the same pronounced periodicities as over the Atlantic. In the eastern Pacific the information flow tends to be quasi-stationary.

Studies of this kind are essential to monitor the performance of the air reporting system. These studies are also of importance in the context of numerical 4-dimensional data assimilation.

1.1.3 Satellite radiance observations

Satellite sounders (NOAA-series) constitute another source of supplementary upper air information especially over oceanic regions.

The observations are made continuously in swaths (25 passes in two days), so that the North Atlantic is covered twice a day.

In the nighttime ascending mode the satellite moves from southeast to northwest, in the daytime descending mode from northeast to southwest (Fig. 6). The observation sequences are made along the orbital path and on two lines parallel to this path, each on a side. At successive days the swaths are being displaced half a pass distance, but every second day the swaths overlap again. The set of network points is quasi-fixed with a spacing of approximately 500 km. But it may occur that observations are missing due to cloud conditions. For the same reason the data points may be off-centred with respect to the nominal positions, so that the data points appear to be irregularly distributed. Three successive passes cover the North Atlantic and the observations are made approximately within 3 hours around the main synoptic hours (00 and 12 GMT). North of 58° N successive swaths overlap each other. South of 58° N some elongated sectors remain uncovered in both the ascending and descending modes. When the data points of satellite soundings interfere with the data points of aircraft observations or radiosonde observations, it is possible by using some diagnostic tools to adjust the observations to those of the other data sources.

1.2 The system mix of radiosonde-, aircraft- and satellite observations

The fundamental principle for an observational system is that the observations convey sufficient and precise information to permit the attainment of the basic goal of data handling and processing. The observational data requirements as specified in the WWW-plan (see Annex) have been established without reference to the composition of the system, be it a single system or an aggregate of different observation systems.

When in a compound system the observational data requirements can be met by each constituent part, then they can be met also by the compound system. On the other hand, if the requirements can

be met in the compound system this need not be the case for each component system.

The observational data requirements contain specifications of the data coverage, the horizontal, vertical and time resolution and the error structure of the available observational material.

In the specification of the observational data requirements account has been taken of the fact that the various parameters defining the large-scale motion of the atmosphere are dynamically coupled. In numerical processing some parameters have been found to be more essential in defining the state of the atmosphere, while others are of secondary importance. Temperature at middle and high latitudes is regarded as a primary parameter, but humidity is only a secondary one. This is not to be interpreted that humidity observations should be of no use. When, for example, the observational material is used in the preparation of charts by graphical methods, no distinction is made between primary and secondary parameters. The dynamical coupling is then taken into account only qualitatively. For practical reasons it is therefore desirable that the data sets of an upper air observation system should comprise at least the following "independent" variables: pressure P, temperature T, wind $\vec{v}$, and relative humidity r. In addition, it is desirable to have the disposal of information on some dependent variables such as geopotential height Φ, dewpoint deficit, etc.

For convenience a data set is considered to be complete, if the set contains information on the following state variables: P, T, $\vec{v}$, r and Φ. Table I summarizes the main characteristics of the data coverage and space-time resolution for the various component systems of upper air observations in the NAT air space. Table II gives a summary of the elements received in TEMP/PILOT, AIREP and SIRS reports together with estimates on the accuracy attainable.

It is obvious that the performance of a mix of observation systems might be evaluated by a careful examination of the performance of each component.

Table I

Data coverage and space-time resolution for three upper air observation systems in the North Atlantic Region.

observational system	coverage		space resolution						time resolution		
			geographical network		data point sets						
					horizontal		vertical		type	peak hrs, main observ. times	main period
	horizontal	vertical	type	specification	type	remarks	type	remarks			
radiosonde/rawin observations (TEMP/PILOT)	WWW network	up to ± 10 mbar	fixed	coastal, island and stationary ship stations	fixed		fixed variable	standard pressure levels significant levels	synoptic	00 (06) 12 (18) GMT	12 hr
aircraft meteorological observations (AIREPS)	commercial air routes	between 300 and 200 mbar	fixed	1° latitude points on 10° meridians	variable	depends on atmospheric circulation and actual traffic pattern	fixed	flight levels	asynoptic	04, 16 GMT	12 hr
satellite radiance observations (SIRS)	orbital swaths	up to 10 mbar	quasi-fixed	side scanning along orbital path	variable	depends on cloud conditions	fixed	standard isobaric levels or layers	asynoptic	00, 12 GMT	12 hr

Table II

Data sets available in TEMP, AIREP and SIRS reports and error structure.

report	para-meter	datum				error structure		
		standard pressure levels	significant levels	flight levels	standard thickness	random errors	others	remarks
TEMP	p	(+)	+			1-3 mbar	systematic	$\pm$ 2° C in
	T	+	+			$\pm$ 1° C	errors	stratosphere
	$\vec{v}$	+	+			$\pm$ 1 m s^{-1}	not	up to 10 m s^{-1}
	r	+	+			$\pm$ 5 %	known	not useful <-40° C
	Φ	+				2-4 %		
	h				(+)			
AIREP	p			+		$\pm$ 1 mbar	systematic	
	T			+		$\pm$ 1° C	errors	
	$\vec{v}$			+		1-2 m s^{-1}	not	
	r						known	INS, Doppler
	Φ							
	h							
SIRS	p						systematic	large errors
	T	+				$\pm$ 2° C	and space-	in clouds
	$\vec{v}$						correlated	
	r						error not	
	Φ						known	
	h				+	0.6°/100 km		larger errors in clouds

Note: p = pressure
T = temperature
$\vec{v}$ = wind velocity
r = relative humidity
Φ = geopotential height
h = thickness
(+) = implicitly available

1.2.1 Data coverage

Fig. 4 shows a map of the upper air observing stations in the WWW-network for the NAT-region. The network includes coastal and island stations as well as the new NAOS-network. The horizontal coverage is very poor. At the stations data are available in sufficient quantity up to about 10 mbar.

The map in Fig. 5 gives an impression of the network of possible AIREP-locations including some near-shore reporting points where a transition is taking place between the oceanic air traffic and the continental air traffic. The points encircled represent the data points retrieved from a set of air reports actually received on 7 January 1975, 12 GMT $\pm$ 4 hours. The coverage should be considered in terms of the actual data point sets, not in terms of the network proper. In the vertical the data coverage is limited to the upper troposphere and lower stratosphere between 300 and 200 mbar.

The map in Fig. 6 shows the nominal SIRS-positions belonging to three orbital swaths in the daytime descending mode on 7 January 1975, 12 GMT $\pm$ 3 hours. Asterisks represent the actual positions of reports received on this date. Although the coverage appears to be reasonable in terms of the scanning geometry, it is questionable whether the coverage in terms of data points may be qualified as being satisfactory. Dependent on the cloud conditions large gaps may occasionally be present in the data point arrays. A compilation of the data point sets for all three subsystems is reproduced in Fig. 7. In combination, the texture of the various data point arrays differs markedly from the texture of the arrays of possible network points. The horizontal coverage in the system-aggregate is at least as good as the coverage for each component separately. The overall coverage occasionally deteriorates substantially, which may be caused by some external factors such as the state of satellite orbiting, the prevailing cloud conditions or the actual route pattern in the organized track system.

The data coverage at intermediate times between the main synoptic hours should be qualified in terms of the coverage of the air

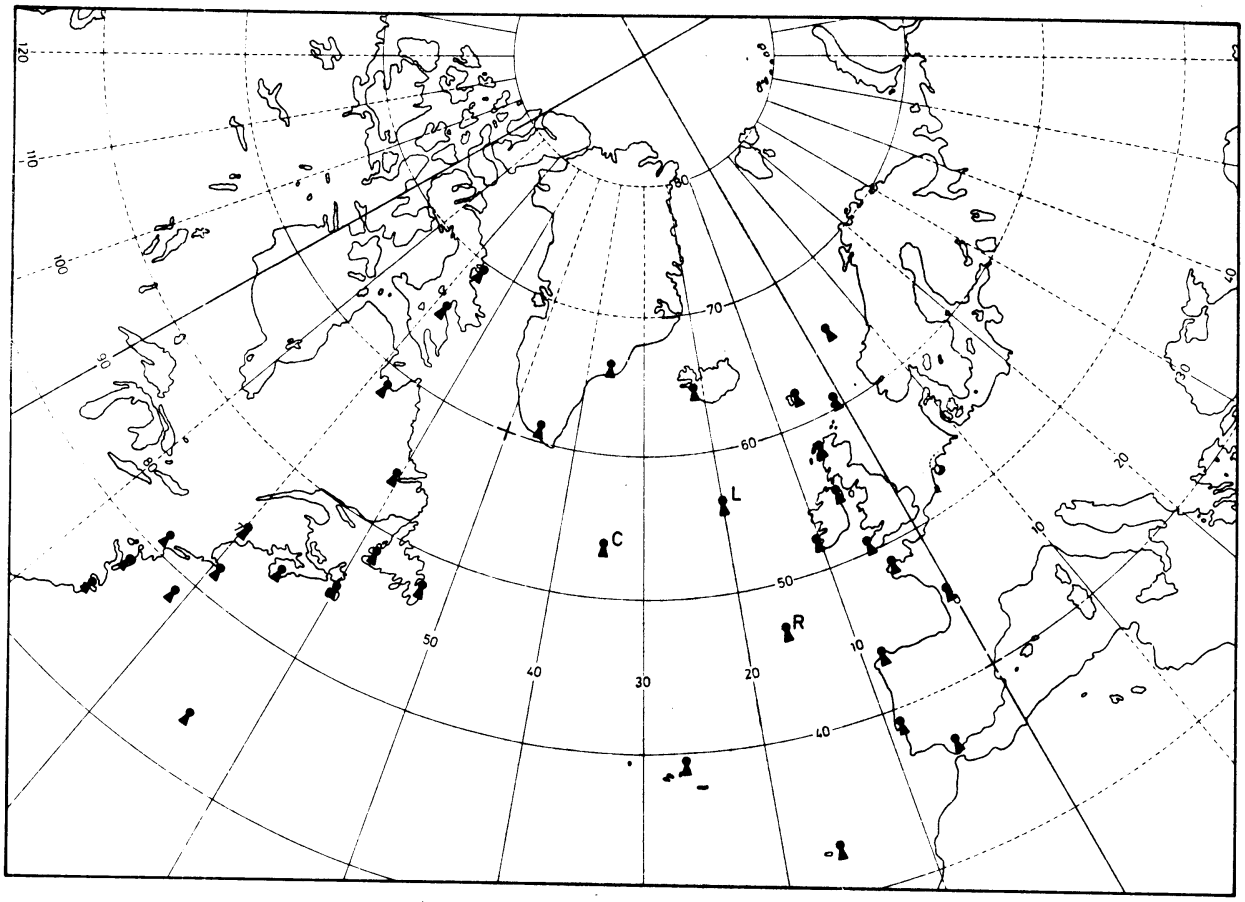

Figure 4 WWW-network of upper air observation stations in the North Atlantic Region.

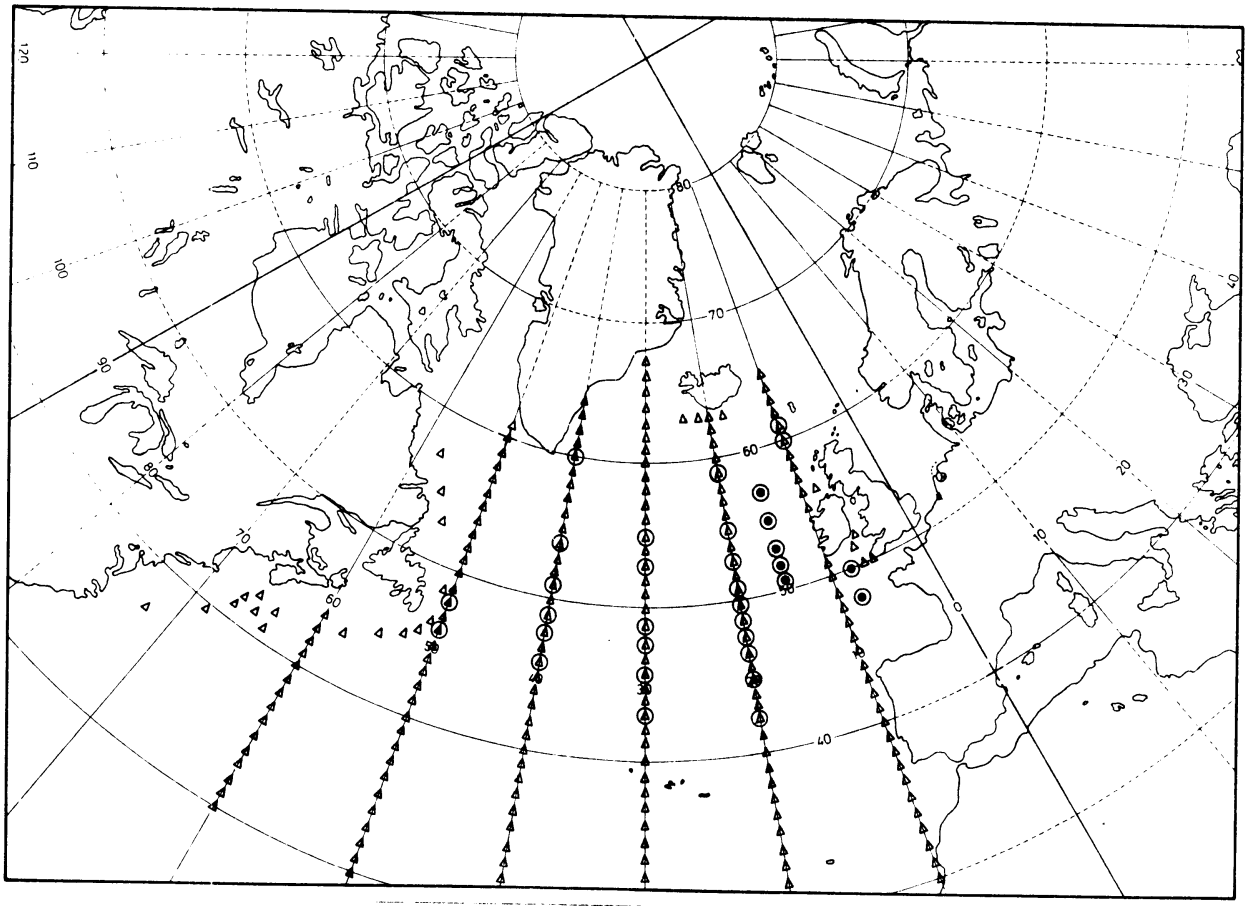

Figure 5 Network of possible AIREP locations in the North Atlantic Region. Open circles represent actual locations on 7 January 1975, 12 GMT ± 4 hours.

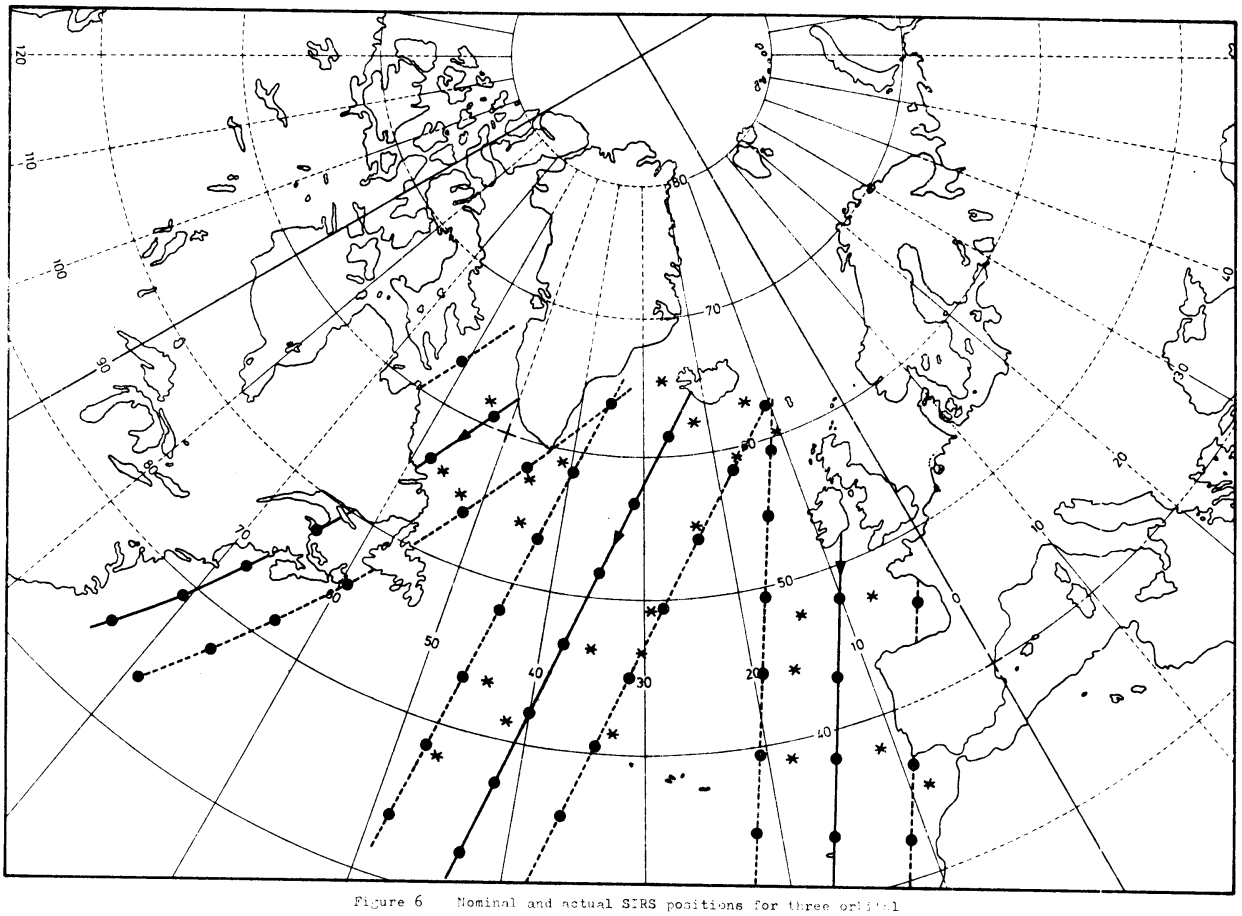

Figure 6 Nominal and actual SIRS positions for three orbital swaths in the daytime descending mode on 7 January 1975, 12 GMT ± 3 hours.

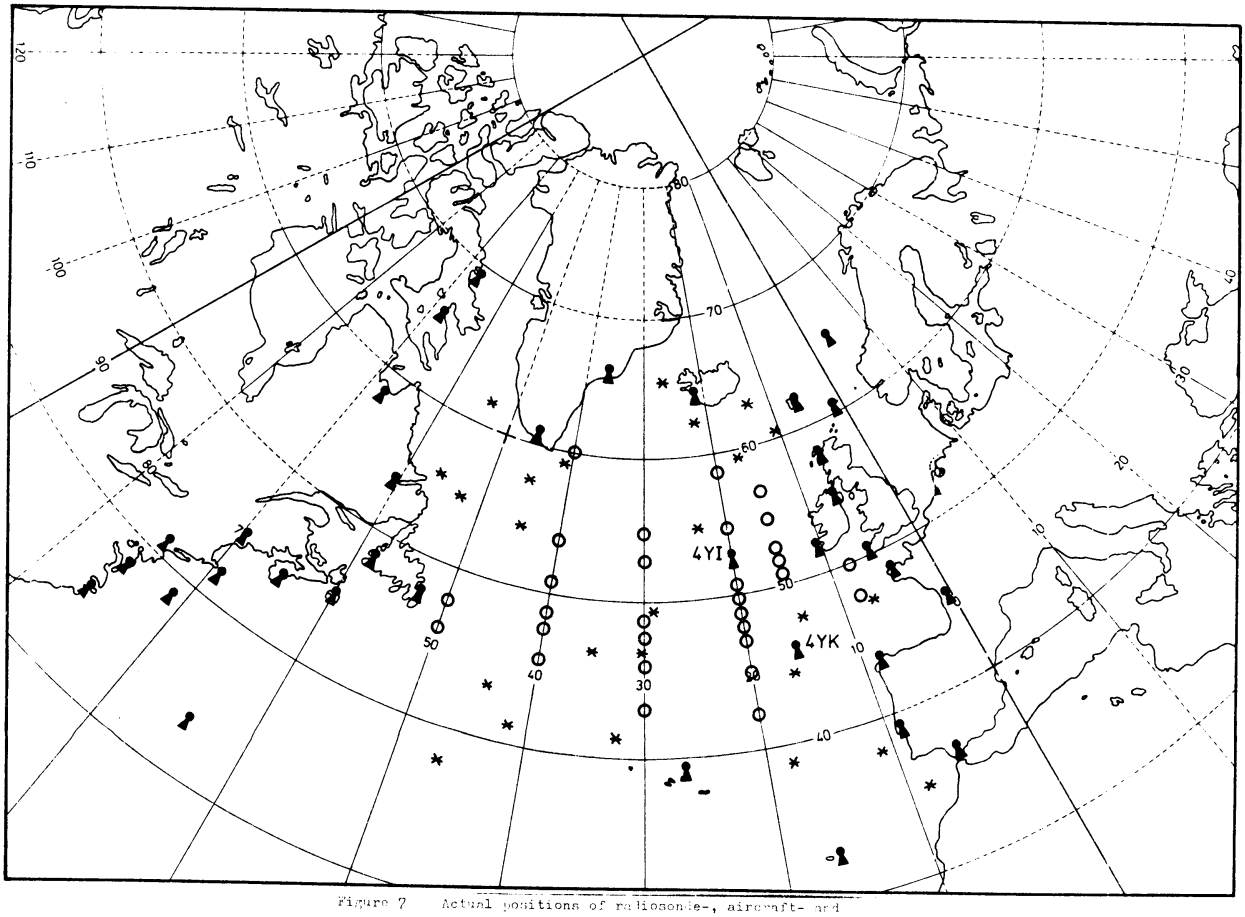

Figure 7 Actual positions of radiosonde-, aircraft- and satellite observations on 7 January 1975, 12 GMT ± 4 hours. ▮ radiosonde station, ⊙ aircraft position, • SIRS position.

reports only, plus some wind observations in the WWW-network at 06 and 18 GMT. The coverage then varies in step with the periodicity of the data supply of these synoptic aircraft observations.

1.2.2 Space-time resolution

In the context of combined data processing a very important item concerns the spatial and temporal resolution of the observations in the system mix.

The space-time resolution in general will be better in an aggregate of observational systems than in each component system separately. As with the data coverage the space-time resolution aspects should be studied in the actual network of data points.

The interpretation of these resolution criteria may be difficult in the case of observational systems which provide a continuous flow of asynoptic data as the air reporting and satellite systems. The interpretation is even more complicated in a system mix as a consequence of multiple data coverage and periodicities in space as well as in time of the various data point arrays.

In general terms the space-time resolution criteria should be specified jointly in models of 4-dimensional data assimilation. This is one of the objectives in GARP-studies. In the present WWW-plan the criteria have been established to apply in the space domain and time domain separately. The discussion to follow is based on this principle.

In the case of separate space-time resolution requirements it is assumed that the observational material is subdivided into samples for time intervals of several hours.

1.2.2.1 Horizontal resolution

The horizontal resolution of observations might be considered as adequate if the distribution of the data points is homogeneous and isotropic and the spacing of the data points is within the limits specified by the minimum observational data requirements.

The spacing and geographic distribution of data points in the WWW-network of upper air soundings are fixed in time, but the resolution in the NAT-region is very poor except in some coastal regions.

In the air reporting system and satellite system not all network points need to be occupied with data, and in the case of satellite soundings the data points may be off-centred with respect to the nominal positions. The distribution of aircraft data points is far from being homogeneous and isotropic. The distribution may even be conceived as being one-dimensional in view of the clustering effect along 10^{o} reporting meridians. The same applies, but to a lesser extent, to the observations along satellite passes.

When the data point arrays of the various systems in a system mix interfere, then the distribution may abruptly change from one-dimensional into two-dimensional. Then at times the density of the network may be sufficient to meet the resolution requirements.

1.2.2.2 Vertical resolution

The resolution in the vertical depends on the levels for which data are available.

In upper air soundings the data points refer to standard pressure levels and significant temperature, humidity or wind levels. For this category of observations the resolution in the vertical is adequate.

The reports of aircraft are linked to standard flight levels. Data points refer predominantly to uneven flight levels (Fl 29, 31,..), a few to even flight levels (cf. section 1.1.2).

The vertical resolution is undefined except when different aircraft happen to report at the same geographic positions, but at different altitudes, within close time limits.

The satellite soundings provide information on 15 standard isobaric levels and 14 layers. The vertical resolution may be qualified as satisfatory.

In a system mix the observational characteristics do not add a new element as to the specification of the resolution in the vertical, because the data points of the various subsystems do not coincide. However the overall space resolution may improve considerably and reach a point where it deserves serious consideration to develop a scheme of combined data processing.

1.2.2.3 Time resolution

It has already been pointed out that there exists a close relationship between the structure of the data point arrays in the space domain and the resolution of the observations in the time domain.

In the system mix in the North Atlantic Region the data supply is composed of

(a) the periodic supply of synoptic radiosonde/rawin observations at the meteorological standard observation times;
(b) the continuous and periodic supply of asynoptic aircraft observations with peaks around 04 and 16 GMT;
(c) the periodic supply of asynoptic satellite observations.

Accumulation of all reports takes place at 04 GMT ± 3h, 12 GMT ± 3h, 16 GMT ± 3h and 00 GMT ± 3h.

From a point of view of combined data processing it is important to look at the data supply in the principal intervals centred about the main synoptic hours.

Within these intervals every two hours a satellite pass provides asynoptic upper air data. Three passes are required to cover the ocean in a time span of 4 to 5 hours. The rate of supply of aircraft meteorological reports is extremely low about the main synoptic hours (00 and 12 GMT). The rate increases towards the ends of the principal intervals.

Because the air reports play a dominant part in the combined data processing, the principal interval should be of considerable length, say, of the order of 6 hours or more. In between the principal intervals the air reporting system is the only data source (except for some rawin reports in the WWW-network at 06 and 18 GMT). In order that valuable information be not wasted, the data might in principle be processed in a model of intermittent or continuous 4-dimensional data assimilation. For a further discussion of this subject we refer to section 2.7.

1.2.3 Accuracy

The accuracy of a data source depends on the error structure of the meteorological parameters it affords. The meteorological parameters are obtained either directly from instruments or indirectly by conversion of raw data such as instruments readings and sensor signals. The accuracy of the observations therefore is not only dependent on the type of instruments and observational technique used, but also on the computational technique. Apart from measurement errors the observational errors include also real fluctuations on a small scale (sampling errors). To obtain representative values for a parameter it is necessary to remove these small-scale fluctuations by a process of time-space averaging, but unfortunately this is not practicable unless the averaging is included in the sensors.

The effect of the computational technique on the error structure is often purely mathematical of origin. Large errors may arise e.g. when a dependent variable becomes very sensitive to small changes in the values of the independent variables near poles of an expression or when the solution of an equation is not unique or when an integration is performed over a domain of measured values including bias. Examples of these error sources are encountered in various subsystems in a system mix. The accuracy of an observation system highly depends on these "natural" errors.

Furthermore, the quality of the reports may be affected by a category of "administrative" errors (incorrect readings, errors in registration and coding) and telecommunication errors. These error sources might probably be eliminated only when suitable automatic data acquisition units and automatic data links are developed and become operative.

It is obvious that in practical operations adequate provisions should be made for quality control of the reports to ensure that the data are as free from errors as possible. Errors may be random, systematic or even be correlated. Systematic errors are primarily due to maladjustments of equipment or to calibration errors. Correlated errors are supposed to exist in the temperature data retrieved from satellite soundings, due to areas of widespread cloudiness.

In a dense network random errors may successfully be suppressed in objective analysis using appropriate interpolation schemes. The removal of systematic errors and in particular of correlated errors is much more difficult. [4,5].

Minimum requirements of accuracy are summed up in the WWW-plan (see Annex) and corresponding estimates are given in table II.

A comparison of accuracies of the various subsystems is of vital importance especially with respect to the combined data processing aspects in a system mix.

Balloon system

The upper air data do not meet the requirements completely. The accuracy of temperature is satisfactory in the troposphere; the temperature error in the lower stratosphere is of the order of 2^{o} C and increases to 2-4^{o} C in the upper stratosphere. Integration of the hydrostatic equation may produce systematic errors in the geopotential, due to bias in pressure and/or temperature. In a network these errors manifest themselves again as random, because they are not space-correlated.

The accuracy of the wind observations depends on the computation technique used to convert balloon positions into wind displacements. Wind data may be derived from the position coördinates afforded by windfinding radars, radiotheodolites or radio direction finders together with altitude information obtained from radiosonde observations. Actually the wind velocity is computed using one of the four possible computational modes. [6].

The wind accuracy resulting from a computation in the "height-elevation" mode deteriorates significantly for large balloon distances (strong winds). Applying the "height-range" mode, the wind error becomes marginal when the balloon approaches zenith. Only when the computation is performed in the "range-elevation" mode or the "range-elevation-height" mode the accuracy of the wind velocity will be satisfactory in the whole operating range.

Small-scale wind fluctuations are difficult to filter out. Some compromise must be found between accuracy and vertical resolution.

Aircraft system

In table II the error estimates of meteorological parameters measured on board aircraft hold for research aircraft equipped with standard instrumentation. [7]. Doppler and INS submit spot winds with a stated accuracy of 1-2 m s^{-1}.

The error in ambient or static temperature as derived from resistance wires, thermocouples, etc. is of the order of $\pm$ 1° C. The manufacturer's specification for accuracy of pressure transducers used to measure ambient or static pressure is $\pm$ 1 mbar. From practical experience it would appear that the figures stated are too optimistic in view of the variable quality of the reports received. It is frequently observed that AIREPs contain large errors. This might be explained by the fact that the air reporting system in its present form presumably is a source of large administrative and telecommunication errors,

because operationally the system requires so many interventions in the making, recording, coding and transmission of the reports.

As wind and temperature are not measured directly, but need a conversion in which some navigational parameters are involved, these elements may also show some bias but the order of magnitude is not known.

Satellite system

The error structure of satellite radiance observations is the most complicated of all and is not fully understood yet.

In recent studies [4,5] three major error sources are indicated: the uncertainty of the mathematical solution of the inverse problem, the uncertainty of molecular absorption data and the contamination of the radiance measurement by clouds and minor gaseous constituents.

The inaccuracy of the observations is more influenced by the process to retrieve the atmospheric temperature profile than by the remote radiance data alone.

First of all it is necessary to emphasize that the inverse radiation equation admits no unique solution. In fact, various temperature profiles can fit the observed radiance data.

By selecting a first guess solution and a specific inversion scheme the number of possible solutions is restricted. Then it is obvious that the error structure is affected by the choice of the first guess temperature field. In practice it has been found that the errors are significantly correlated with the first guess field errors ($\sim$ 0.5-0.7). Especially when the actual forecast is used as a first guess the running forecast is correlated with the observations, so that the error may gradually grow to very large values especially in data-sparse areas. In a model of 4-dimensional data assimilation correlated errors have a more serious impact than uncorrelated errors. Other errors due to erroneous calibration of channel transmittance or to contamination effects by clouds or water vapour are also very noticeable. Evidence has also been reported of a significant correlation of the retrieval error and prevailing weather systems.

1.3 Observational data requirements in the system mix

In the WWW-plan minimum observational requirements have been specified based upon extensive preparatory studies for GARP. These studies show the influence of two factors: (1) the capability of users to apply the data either manually or through numerical models, and (2) the capability of the observing systems.

In the previous sections we have made an analysis of the observational characteristics of the various subsystems of upper air observations and the system mix as a whole in the NAT airspace. In addition, attention has been paid to what degree these observational characteristics meet the recommendations in the WWW-plan.

It was observed that the observational characteristics in the system mix could not be specified merely by taking together the observational characteristics for the various subsystems. For example the horizontal resolution in the network of data points in the system mix proved to be much better than the resolution of networks of data points associated with the component systems separately. Some data requirements could be met in the system mix where the subsystems were in default. None of the observation systems of upper air data in the NAT-region fully meets the data requirements as stated in the WWW-plan. In the system mix by a blending of data coverage, space-time resolution and other attributes the criteria can be met more closely, but whether they fully meet the requirements remains an open question. This is attributable to the fact that it is not possible on scientific considerations to specify fully the optimum requirements for the spacing and accuracy of asynoptic observations conveyed by such data sources as the air reporting and satellite systems. The complexity of the problem is clearly reflected in the network of data points in the system mix by the variability of data coverage, space-time resolution, etc. due to the periodicities both in the space-domain and time-domain. In future data requirement studies

account should be taken of the capability of the various observing systems in a system mix as a whole and the effectiveness of the observational programmes to permit the attainment of the basic goal of meteorological data processing. In this context special attention should be paid to the aspects of pre-analysis processing, numerical analysis and prediction, the problem of initialization and models for 4-dimensional data assimilation.

-o-o-o-

PART II

2. Pre-analysis processing in a system mix

In various approaches to the problem of numerical integration of the physical prediction equations which govern the large-scale motions of the atmosphere a limited amount of primary data is required in order to define the initial state of the motions at standard observation times.

In a hydrostatic system the observed variables of primary importance needed to close the system of equations are surface pressure (pressure on other levels), temperature, horizontal wind components and humidity.

Other (secondary) data need not be observed as they can at least in principle be derived from the primary data, using some dynamical and physical constraints.

Most of the elements needed are present in the data sets conveyed by the upper air observation systems, which are operative in the North Atlantic Region. From a point of view of data processing either manually or through numerical models the available data sets should preferably be complete in the sense as discussed in section 1.2. However, as can be inferred from table II, most data sets have some parameters missing, for example geopotential and humidity in aircraft reports and wind velocity and humidity in satellite reports. This poses the problem whether the incomplete data sets may be replenished with some missing data through the use of diagnostic tools in the network of data points associated with the system mix.

Another important item concerns the necessity that the data should be linked to meteorological standard (pressure) levels. This is actually the case with data conveyed by the radiosonde- and satellite observations, but the data extracted from aircraft reports, which are linked to standard flight levels, need a process of selection and interpolation to the nearest standard pressure levels.

These two examples clearly show that the primary data should first be subdued to a form of pre-analysis processing before they are suited to be applied in the integration of the state equations.

This chapter introduces a new method to solve this "combined processing" problem in a network of data points associated with the system mix of upper air observations in the North Atlantic Region.

2.1 Computation of the absolute geopotential in a system mix

To extend incomplete data sets with additional values of missing parameters the values should be derivable from the measured data of some independent variables. The only element in the data set which suits this purpose is the geopotential height. This parameter is missing in aircraft reports. In satellite reports, to obtain the absolute geopotential, the reported values of geopotential thickness need to be updated using some tropospheric reference value.

The geopotential associated with an aircraft position might in principle be evaluated within the network of data points of radiosonde and aircraft observations. Prerequisites for this are the availability of some dynamical and physical constraints and some geopotential reference values. Suitable reference values can be obtained from radiosonde reports. A useful diagnostic tool is available in the form of a "geopotential theorem" to be described in the next section.

The method which we propose to acquire "aircraft geopotentials" is based upon the following procedure:

(1) First a selection is made of reports of radiosonde-, aircraft- and satellite observations, which are valid in a principal time interval centred about the main synoptic hour.

(2) Next, within the network of data points of radiosonde- and aircraft observations the aircraft geopotential is computed by application of the geopotential theorem.

(3) The aircraft geopotentials are updated to obtain absolute geopotentials using the absolute geopotential of radiosonde observations as reference or calibration values.

(4) Next, a process of correction is initiated to suppress deviations of the computed and measured geopotentials in the data points of radiosonde stations.

(5) Finally, the aircraft geopotentials are interpolated to the nearest standard pressure levels.

(6) From the geopotential thickness values contained in satellite reports the absolute geopotentials are determined using the radiosonde- or aircraft geopotentials as reference.

The geopotentials thus obtained in a scheme of combined processing in the system mix contribute to a better definition of the initial state of the atmosphere. The material may immediately be used as input data for a numerical model of objective analysis and prediction or simply as extra information for the manual preparation of charts.

2.2 A geopotential theorem

In an elementary application of the equation of horizontal motion a special integral theorem may be formulated, which can be utilized as a powerful diagnostic tool for various purposes especially to derive the "aircraft geopotential" in a mixed observation system [8].

In mid-latitude synoptic scale systems the wind and pressure fields are in approximated geostrophic balance. In vector form this balance may be expressed as

$$f \vec{v}_g = k \times \frac{1}{\rho} \nabla_z p \qquad (2.2.1)$$

where $\vec{v}_g$ is the geostrophic velocity and $\nabla_z p$ the horizontal pressure gradient.

$f = 2\Omega \sin\varphi$ is the Coriolis parameter;

Ω = the angular speed of rotation of the earth;

φ = latitude;

ρ = density;

$\vec{k}$ = a unit vector pointing to zenith.

In isobaric coördinates the vectorial form of the geostrophic relationship is:

$$f \vec{v}_g = g \vec{k} \times \nabla_p z \equiv k \times \nabla_p \Phi \qquad (2.2.2)$$

g = the acceleration of gravity;

Φ = the geopotential defined as the work required to raise unit mass from the surface to the height z;

$\Phi = \int_0^z g \, dz$

To represent the atmospheric flow in arbitrary surfaces, which are not level, we shall have to derive the horizontal pressure gradient along the surface.

Let Σ be an arbitrarily defined sloping surface in the atmosphere. The surface Σ is specified by some scalar quantity S = const. The surface Σ is a physical surface if S represents a physical parameter.

Consider a cross section in the (xz) plane. Then the following holds:

$$\left(\frac{\partial p}{\partial x}\right)_z = \left(\frac{\partial p}{\partial x}\right)_S - \left(\frac{\partial p}{\partial z}\right)\left(\frac{\partial z}{\partial x}\right)_S \qquad (2.2.3)$$

The subscript S means "holding S constant".

If we substitute on the right from the hydrostatic equation and introduce the geopotential, we obtain:

$$\left(\frac{\partial p}{\partial x}\right)_z = \left(\frac{\partial p}{\partial x}\right)_S + \rho \left(\frac{\partial \Phi}{\partial x}\right)_S$$

A similar equation may be written for a cross section in the (yz) plane.

These equations relate the horizontal pressure gradient force per unit mass to the pressure gradient force per unit mass on the surface.

In vectorial form:

$$\nabla_z p = \nabla_S p + \rho \nabla_S \Phi \qquad (2.2.4)$$

where $\nabla \equiv i \frac{\partial}{\partial x} + j \frac{\partial}{\partial y}$ denotes the horizontal gradient operator.

When Eq. (2.2.1) and Eq. (2.2.4) are taken together, then the result is the appropriate form of the geostrophic relationship in the Σ surface:

$$f \vec{v}_g = k \times \nabla_S \Phi + \frac{1}{\rho} k \times \nabla_S p \qquad (2.2.5)$$

Let Σ be the support of an arbitrarily chosen curve Γ connecting the points P and Q located on the surface. Then we consider the line integral:

$$\int_{\Gamma P}^{Q} f \, [k \times d\vec{s}\,] \, \vec{v}_g \qquad (2.2.6)$$

where $\vec{s}$ defines the integration path.

Substitution of Eq. (2.2.5) in Eq. (2.2.6) yields:

$$\int_{\Gamma P}^{Q} f \, [k \times d\vec{s}] \, \vec{v}_g = \int_{\Gamma P}^{Q} f [ds \times \vec{v}_g \,] \vec{k}$$

$$= \int_{\Gamma P}^{Q} (ds \times [k \times \nabla_S \Phi]) \, \vec{k} + \int_{\Gamma P}^{Q} \frac{1}{\rho} (d\vec{s} \times [k \times \nabla_S p]) \, \vec{k}$$

In view of the vector rule

$$a \times [b \times c] = (\vec{a}.\vec{c}) \, \vec{b} - (\vec{a}.\vec{b}) \, \vec{c} \quad \text{we have}$$

$$\int_{\Gamma P}^{Q} f [d\vec{s} \times \vec{v}_g \,] k = \int_{\Gamma P}^{Q} (d\vec{s}. \nabla_S \Phi) \, (\vec{k}.\vec{k}) - \int_{\Gamma P}^{Q} (d\vec{s}.\vec{k}) \, (\nabla_S \Phi . \, k)$$

$$+ \int_{\Gamma P}^{Q} \frac{1}{\rho} (d\vec{s}.\nabla_S p) \, (\vec{k}.\vec{k}) - \int_{\Gamma P}^{Q} \frac{1}{\rho} (\vec{ds}.\vec{k}) \, (\nabla_S p.\vec{k})$$

Observing that

$$\vec{k}.\vec{k} = 1$$

and $$\vec{k}.\ \nabla_S \Phi = 0$$

$$k.\ \nabla_S\ p = 0$$

the expression on the right can be written:

$$\Gamma\int_P^Q \nabla_S \Phi\ .\ d\vec{s} + \Gamma\int_P^Q \frac{1}{\rho}\ \nabla_S\ p.\ d\vec{s}$$

but $$\Gamma\int_P^Q \nabla_S \Phi\ .\ d\vec{s} = \Gamma\int_P^Q d_\Gamma \Phi = \Phi_Q - \Phi_P$$

and $$\Gamma\int_P^Q \frac{1}{\rho}\ \nabla_S\ p\ .\ ds = \Gamma\int_P^Q \frac{d_\Gamma\ p}{\rho}$$

The index Γ indicates here that the increments in Φ and p have to be taken along the curve Γ. In a local (xyz) coördinate system the integrand $f\ [ds\ x\ \vec{v}_g]\ \vec{k}$ takes the form $f\ (v_g\ dx - u_g\ dy)$. The integral (2.2.6) can best be expressed in a fixed Cartesian coördinate system referring to a conformal map projection. The integral then becomes

$$\Gamma\int_P^Q \frac{f}{m}\ (v_g\ dx - u_g\ dy) \qquad (2.2.7)$$

where m is the map factor. For instance, in a conformal polar stereographic projection $m = \frac{2}{1 + \sin \varphi}$.

Furthermore, by substituting from the equation of state for moist air:

$$p = \rho\ RT_v,$$

where R is the gas constant for dry air and T_v the adjusted virtual temperature, we finally obtain the following expression:

$$\boxed{\Phi_Q - \Phi_P = \Gamma\int_P^Q \frac{f}{m}\ (v_g\ dx - u_g\ dy) - \Gamma\int_P^Q RT_v\ d\ \ln\ p} \qquad (2.2.8)$$

This expression permits the computation of the geopotential along an arbitrary curve in the atmosphere when sufficient information on pressure, temperature, humidity and wind along the curve is known, and in addition a reference geopotential value is available at least in one point. This "geopotential theorem" holds within a geostrophically approximated air motion at a fixed time. The theorem admits various interpretations, dependent on its use in selected applications. Specializations of the theorem offer the possibility to derive well-known diagnostic relations in dynamical meteorology, e.g. the thermal wind equation and the Montgomery stream function valid for isentropic surfaces.

Obviously, the theorem is particularly suited to be used in series of consecutive observations, provided by upper air soundings, dropsondes, constant level balloon flights and long-range flights of commercial aircraft.

Upper air soundings

Let the integration path Γ be the trajectory of a balloon flight of an upper air sounding. The balloon drifts freely with the wind.

Therefore $\quad v\,dx - u\,dy \equiv 0$

Assuming that the wind $\vec{u}$ is in the direction of the geostrophic wind Eq. (2.2.8) becomes:

$$\Phi_Q - \Phi_P = \Gamma\int_P^Q RT_v \, d \ln p \qquad (2.2.9)$$

This is the basic expression used in the processing and coding of operational radiosonde observations. The same reasoning is valid for dropsondes and constant level balloon flights. When a super pressure balloon moves in a surface of constant density, then Eq. (2.2.8) reduces to the simple form:

$$\Phi_Q - \Phi_P = \Gamma\int_P^Q \frac{dp}{\rho} = (RT_v)_P - (RT_v)_Q$$

Aircraft observations

Let Γ be the flight path of a commercial aircraft equipped with instrumentation to measure wind, temperature and pressure, and let these parameters be sampled at a fairly high rate. Then, at cruising altitude (constant pressure altitude) Eq. (2.2.8) becomes

$$\Phi_Q - \Phi_P = \Gamma\int_P^Q \frac{f}{m} (v_g \, dx - u_g \, dy)$$

By entering the measured wind in this equation a good estimate is found for the height profile along the flight track, provided that the geopotential is known at least at one point of the track. Such a reference value may be available using information from another data source in the system mix.

Eq. (2.2.8) may also be applied when the path includes portions of non-level flight. This requires the availability of the virtual temperature T_v. The aircraft observations however do not submit information on the humidity parameter, so that T_v is not known. In the jet corridor, say, between 200 and 300 mbar, the virtual temperature increment T_v-T amounts to a few tenths of a degree even with 100% relative humidity, so that it is permitted to replace T_v by the reported (static air) temperature T in Eq. (2.2.8).

Pressure data may be derived from the reported level or pressure altitude, which is the altitude corresponding to a given pressure in the ICAO standard atmosphere with a sub-scale setting of 1013.25 mbar (QNE).

In aviation long-range flights and thus the integration paths are under control of some special navigational procedures. The geopotential theorem may then be used to specify properties of the controlling factors. Well known is the principle of single heading flight. Application of the geopotential theorem then leads to the formulation of the well-known drift formula of Bellamy.

Numerical evaluation

Let the integration path be a curve passing through a sequence of data points. Let these data points be numbered by $i = 0...N$. $i = 0$ refers to point P, $i = N$ to point Q. Then Eq. (2.2.8) may be approximated by a stepwise summation and be written in the following linearized form:

$$\Phi_Q - \Phi_P \simeq \sum_{i=0}^{N} \tfrac{1}{2} \left[\left(\frac{f}{m} v_{g,\perp}\right)_i + \left(\frac{f}{m} v_{g,\perp}\right)_{i+1}\right] \Delta s_i$$

$$+ R \sum_{i=0}^{N} \tfrac{1}{2} \left[(T_v)_i + (T_v)_{i+1}\right] \ln \frac{p_{i+1}}{p_i} \qquad (2.2.10)$$

Here $v_{g,\perp}$ denotes the component of the geostrophic wind velocity normal to a great circle arc connecting the geographic positions of the points i and i+1. Δs_i is the length of this great circle arc (Fig. 8).

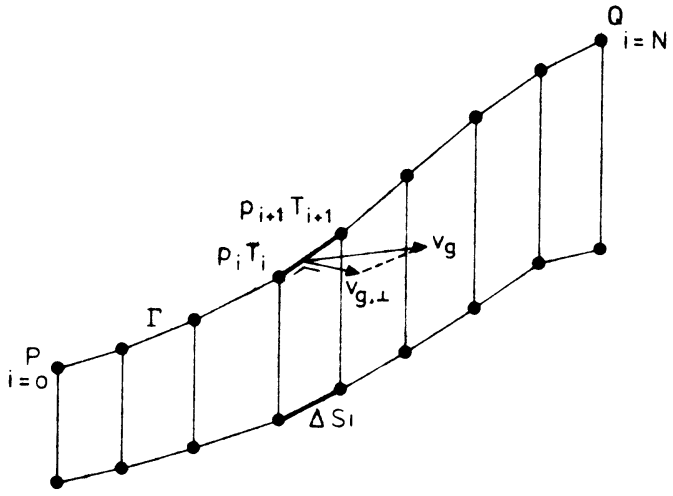

Fig. 8. Calculation of the line integral Eq. (2.2.10) along a path through a sequence of data points.

The accuracy of the computed geopotential using Eq. (2.2.10) depends on a whole scala of uncontrollable factors such as the spacing of data points, the approximation of the wind and virtual temperature by the reported wind and temperature, the effect of discontinuities (fronts, tropopause) on the linearization of terms, the effect of ageostrophic winds and instrumental errors. In particular in the airspace covered by the aircraft observations, between 200 and 300 mbar, the influence of some of these factors may become excessively high, so that the accuracy of the computed geopotential may indeed become marginal. Under unfavourable conditions the error in the computed geopotential may become of the order of 10 gpdam, which is in excess of the estimated RMS error of radiosonde geopotential data (3 to 6 gpdam), so that there is no other way out of the dilemma than to check the computed geopotential against those values reported for upper air soundings and to correct the "aircraft geopotential" accordingly.

On closer examination of the theorem it might be observed that the theorem also admits an interpretation in a 3-dimensional network of data points. This requires the introduction of a graph structure in the network and the definition of a suitable path structure to evaluate Eq. (2.2.8) or Eq. (2.2.10) in all data points. A discussion of the generalization of the theorem and its application in a system mix forms the main subject of the remainder of this report.

2.3 Pre-analysis processing of aircraft meteorological reports

We have seen that the primary data contained in the reports of aircraft observations do not comprise a "complete set" as required for the purpose of chart preparation or numerical analysis. There is a need to extend the data set with missing parameters and to interpolate the reported values to adjacent meteorological standard levels. Parameters which are missing in AIREPs are humidity and absolute geopotential. Only the

latter element, being a dependent variable, might be derived from the reported parameters in the system mix, using some suitable diagnostic relation.

2.3.1 Aircraft potential

To obtain valuable geopotential data in the aircraft positions a method is proposed which is based on a stepwise approach as indicated in section 2.1. The method is centred about an application of the geopotential theorem in the 3-dimensional network of data points in a mix of upper air and aircraft observations. The upper air stations figure as calibration stations, and the geopotential values obtained from the upper air soundings serve as error-free reference values to check the computed geopotential by means of Eq. (2.2.8).

The path integration of Eq. (2.2.8) in a 3-dimensional network of data points requires the definition of a well-ordered path structure including all data points, so that the computation leads to the presentation of a unique set of geopotential data in the data points. It is of no sense when the path integration would be performed haphazardly between any pair of radiosonde data points in view of the large multitude of admissible paths and the multiple valued geopotentials resulting from the integration along such paths, in each aircraft position. The problem to determine a well-defined path structure for the integration of expression (2.2.8) immediately suggests that it should be required to introduce a geometric structure in the network of data points and to consult some principles of graph theory. To that aim we need a convenient visualization of the most elementary concepts and structures in a geometric graph.

2.3.1.1 Some basic concepts of geometric graphs

The terminology and symbolism currently in use in graph theory is not standardized. The reader may consult various textbooks [9,10,11] to find suitable vocabularies for describing graphs.

In this section a summary is given of those graph theoretical concepts which play a part in the application of the theorem and the space quality control to be discussed in section 2.4.

The graph structure we have in mind consists of the data points (vertices) interconnected by a system of curves (edges). Because we are interested in the geometric distance of these curves, this geometric structure belongs to the class of geometric graphs. The graph is conceived as an undirected graph, although it should be kept in mind that it may be necessary in some special applications to associate a direction or orientation to the edges. For example, in the problem under consideration the integration along a path may be facilitated by associating a sense of direction with the path. However, since the path may be traversed in both directions, the concept of a directed graph is not relevant here. The vertices connected by an edge are said to be its endpoints. If the endpoints coincide we have a loop. Edges (arcs in a directed graph) are adjacent edges if they have at least one common endpoint. A vertex is said to be isolated if there are no edges incident with the vertex in the graph.
A chain (path in a directed graph) is a finite sequence of adjacent edges (arcs), which form a continuous route.
A circuit (cycle in a directed graph) is a chain which is closed.
A simple chain is a chain in which all vertices are distinct.
A simple circuit is a simple chain which is closed.
A graph is said to be complete if every two distinct vertices in the graph can be joined by an edge.
A graph is said to be connected if every pair of distinct vertices are joined by at least one chain. Other graphs are said to be disconnected. A connected subgraph is called a component of the graph. An isolated vertex is a trivial case of a component of a graph. In a graph a vertex is called a root if all vertices of the graph can be joined by a chain starting at the root.

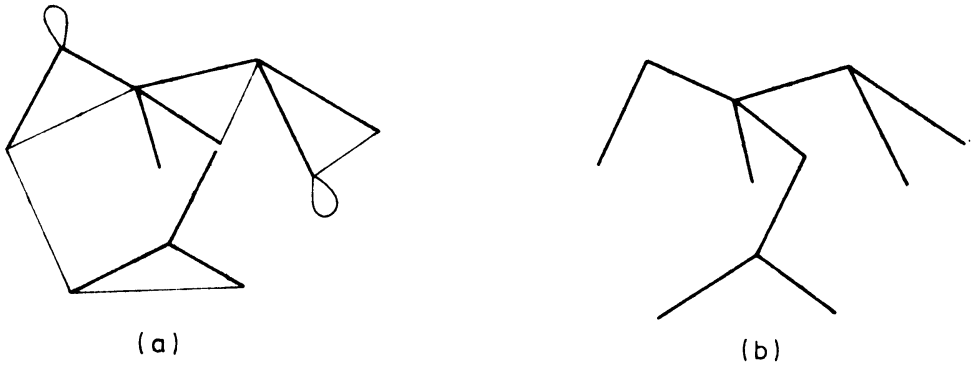

Fig. 9. Geometric graph (a) and tree structure (b).

Very important is the concept of a tree or forest. (Fig. 9). A graph is said to be a tree if it is connected and has no circuits. A graph which is free from circuits and consists of a finite number of components is referred to as a forest. Every tree with n vertices has precisely n-1 edges, and a forest of k trees, which has n vertices, has precisely n-k edges. There exist trees that have a root (arborescences).

The concept of a tree plays a central role in the probem of combined processing in a system mix. A graph is also a tree if and only if every pair of distinct vertices are joined by precisely one chain (path). The removal of any one edge of a tree yields a disconnected graph. The edges of a graph which appear in a tree are called branches relative to a tree, and the edges not included in the tree are called chords relative to the tree.

If all vertices of a graph are included in the tree, the tree is said to be a spanning tree. It is clear that only a connected graph contains spanning trees. Any chord in a tree creates a circuit. The circuits so generated by the chords are independent (they contain an edge not contained in any of the others). These circuits constitute a circuit basis from which any other circuit can be derived in an algebraical context by a linear combination of the independent circuits, which define the circuit basis. The number of circuits in a circuit basis is $m - n + p$, where m is the number of edges of the graph, n the number of vertices and p the number of (connected) components of the graph.

In the class of geometric graphs we are interested in two specially defined trees: the shortest distance tree and the shortest spanning tree.

To define a shortest distance tree it is necessary to consider the well-known shortest path problem. In a geometric graph each edge has an associated positive real number, its distance l(u). The problem is to find a simple path between two vertices that minimizes $\sum_{(u)} l(u)$. The path which solves this problem is called a shortest path. All shortest paths between a given vertex and all other vertices in a graph constitute a rooted shortest distance tree. In general there exists no spanning tree which contains all shortest paths between its vertices, simply because the shortest paths between any pair out of three vertices in such a tree may form a circuit.

A spanning tree of a graph with a minimum total length is called a shortest spanning tree. This tree consists of the n-1 shortest edges of a (connected) graph, which do not form circuits.

2.3.1.2 Selection of an integration path structure

We now proceed with the selection of a path structure which is most suited to be used for the integration of the geopotential formula (2.2.8). First we construct a geometric graph associated with the set of data points of both the upper air soundings and the aircraft observations. The data points figure as vertices of the graph. The edges consist of straight line segments connecting a pair of vertices. However, not every pair of vertices need to be interconnected, because the spacing of data points should remain below a preset threshold value. Otherwise the summation to be performed using Eq. (2.2.10) would become too inaccurate. The threshold value is of the order of the maximum spacing as established in the WWW observational requirements.

The graph thus obtained is therefore in general not complete and also in general not connected. So the graph may possess a limited number of connected components dependent on the actual space distribution of data points. Some data points may even become isolated vertices in the graph.

Next, for the evaluation of the geopotential theorem we like to define a path structure in the graph, which delivers a unique set of geopotential values in all data points. Given n data points in a connected graph, the integration path structure then should contain precisely n-1 edges. Thus we arrive at the conclusion that the path structure should consist of a (spanning) tree. We would have arrived at the same conclusion, if we had stated the requirement that the path structure should contain one single path between any pair of vertices in the graph.

Note: In actual practice when the graph is disconnected the integration is to be performed in a forest. The integration of Eq. (2.2.8) in a forest will indeed convey useful aircraft geopotentials if the connected components (trees) in the forest contain at least one vertex associated with a radiosonde data point as a reference. Otherwise the theorem affords only relative geopotential data in such a tree component.

Each graph is the support of a great multitude of trees. According to a theorem due to Cayley (1897) [12] the number of trees amounts to n^{n-2}. Of course the number of spanning trees is less, but this does not alter the fact that the collection of possible path structures is still extremely large. Then we need to make an additional choice from the collection of spanning trees to find one which is most suited for the path integration. It is not easy to find a criterion which should govern this additional tree selection.

The spanning tree to be selected should contain all shortest edges of the original graph, but then the paths between any pair of vertices are not shortest paths. We also could demand

that the paths in the spanning tree need to be shortest paths, but then these paths are not necessarily composed of shortest edges. The tree involved in the first approach is nothing but the shortest spanning tree as defined in section 2.3.1.1.

In the second approach the shortest distance tree would play a part. These are rooted trees. What we really need is however an unrooted spanning tree in which each pair of vertices is connected by a shortest path (chain), but such a tree does not exist. (Cf. section 2.3.1.1).

Intuitively it is clear that the first approach is to be preferred, not only for the reason just explained but predominantly because by taking the smallest integration steps more accurate intermediate geopotential values may be obtained in the vertices of the graph.

For this reason it is plausible that the shortest spanning tree is the best path structure to be selected for the evaluation of the geopotential theorem.

2.3.1.3 Algorithm for the evaluation of the geopotential theorem in a shortest spanning tree

The algorithm to be developed for the evaluation of the geopotential theorem in the graph should at least comprise two computational procedures: one for the construction of the shortest spanning tree (forest) and one for the integration of Eq. (2.2.8) in the corresponding path structure. Both processes may run independently of each other, but it is more convenient that both processes run in parallel.

In general the construction of the shortest spanning tree is based on the systematic stepwise extension or deletion of a connected or disconnected subgraph. Parallel processing is only feasible when at each step the subgraph remains connected.

To date three or four algorithms are known to be applicable for the construction of the shortest spanning tree. Formally the simplest algorithm is one due to Kruskal [13]. First,

one orders the edges of the original graph according to increasing lengths. Then, starting with the smallest edge, the edge next in length is added, provided that no circuit is formed, and so on until the subgraph contains exactly n-1 edges. This procedure admits no parallel processing of Eq. (2.2.8), as the subgraph in general does not remain connected during the process.

In a dual approach one may proceed by deleting step by step those largest edges from the graph, which do not disconnect the graph. This method is not suited either to include the parallel processing of Eq. (2.2.8), because the deleted subgraph is in general disconnected during the process.

By far the most promising method is one proposed by Dijkstra [14]. Here the construction of the shortest spanning tree makes use of the following two steps repeatedly:

step 1 given the subtree resulting from the preceding two steps, find the smallest of all edges connecting vertices in the subtree with vertices outside the subtree;

step 2 extend the subtree by adding this smallest edge.

The process starts at an arbitrarily chosen vertex and terminates when there are no vertices left outside the subtree.
The shortest spanning tree is thus created by a stepwise extension of a connected subtree. This affords the possibility to compute Eq. (2.2.8) in parallel with the construction of the tree merely by adding the following step:

step 3 compute the geopotential difference along this shortest edge using Eq. (2.2.8).

Now let the vertices of the graph associated with the data points be numbered by $i = 1...n$ and let the radiosonde data points - there may be more data points for reference than radiosonde stations - be indicated by the index i_j $(j = 1...k)$. Then we start the construction of the shortest spanning tree at an arbitrarily chosen vertex, say, $i = 1$, and tentatively

assign to this vertex a zero value for the geopotential height ($\Phi'_{i=1} = 0$). The calculation of the geopotential takes place in step with the tree construction. After termination of the process the computed geopotential data Φ'_i still refer to the initial zero value at the starting point. To obtain absolute geopotentials the relative geopotential data should be matched with at least one reported radiosonde reference value. To update the computed values Φ'_i in reference to one of the reported values Φ_{i_j}, say, for $j = \rho$, the absolute geopotential is obtained by taking

$$\Phi_i = \Phi'_i + \Phi_{i_{j=\rho}} - \Phi'_{i_{j=\rho}} \qquad (i = 1...n)$$

If the theorem would hold unconditionally, then it is immaterial which of the reported radiosonde geopotentials is used as a reference. However, for reasons explained earlier Eq. (2.2.8) is only very approximately fulfilled in the atmosphere. This causes the values Φ_i to deviate from the reported radiosonde geopotentials.

In order to obtain as yet consistency in the geopotential field data it is proposed to proceed as follows.

First we update the Φ'_i values in reference to all reported radiosonde geopotential data:

$$\Phi''_i = \Phi'_i + \frac{1}{k} \sum_{j=1}^{k} (\Phi_{i_j} - \Phi'_{i_j}) \qquad (i = 1...n) \qquad (2.3.1.3.1)$$

These updated geopotential data still deviate from those reported in the radiosonde data points. Then, in order to remove the mis-matching, the off-set values are redistributed over all vertices in the tree by applying a correction of the form

$$\Phi'''_i = \Phi''_i + \frac{\sum_{j=1}^{k} \frac{1}{(a_j)^l} (\Phi_{i_j} - \Phi''_{i_j})}{\sum_{j=1}^{k} \frac{1}{(a_j)^l}} \qquad (i = 1...n) \qquad (2.3.1.3.2)$$

where $\frac{1}{(a_j)^l}$ denotes a weighting factor. a_j represents some distance function between vertex i and a reference vertex i_j of an upper air sounding i_j.

Obviously the corrected geopotential values Φ_i''' take on exactly the reported geopotential values in the k radiosonde data points where $a_j = 0$.

a_j may simply represent the Cartesian distance of the vertex i to the vertex i_j. a_j may also denote the length of the shortest path in the graph between these points or even be the length of the path in the shortest spanning tree between these points. l is an adjustable exponent to change the influence of the points on the correction to be applied. The choice of appropriate weighting factors might best be done empirically.

In case the original graph is disconnected the algorithm may be applied within each connected component. The algorithm which embraces a procedure of path integration in a tree and a procedure which matches the result to some calibration values is very fast on a computer.

2.3.2 Interpolation to standard pressure levels

After the data sets of aircraft observations have been extended with information on the geopotential in the aircraft location the problem remains to relate the computed and reported data to meteorological standard levels. To that aim the data need to be subjected to a form of post-processing including an additional selection and interpolation before they are suited to be inserted in further graphical or numerical processing schemes.

The cross-section in Fig. 10 shows very schematically the isotherms and isotachs in the vicinity of a polar front within the airspace occupied by the air traffic over the North Atlantic. Inserted is also the set of flight levels and the set of standard pressure levels (300, 250, 200 mbar). From a meteorological point of view the airspace under consideration is characterized by excessive wind- and temperature gradients as well as sharp temperature discontinuities (front, tropopause) and wind extremes

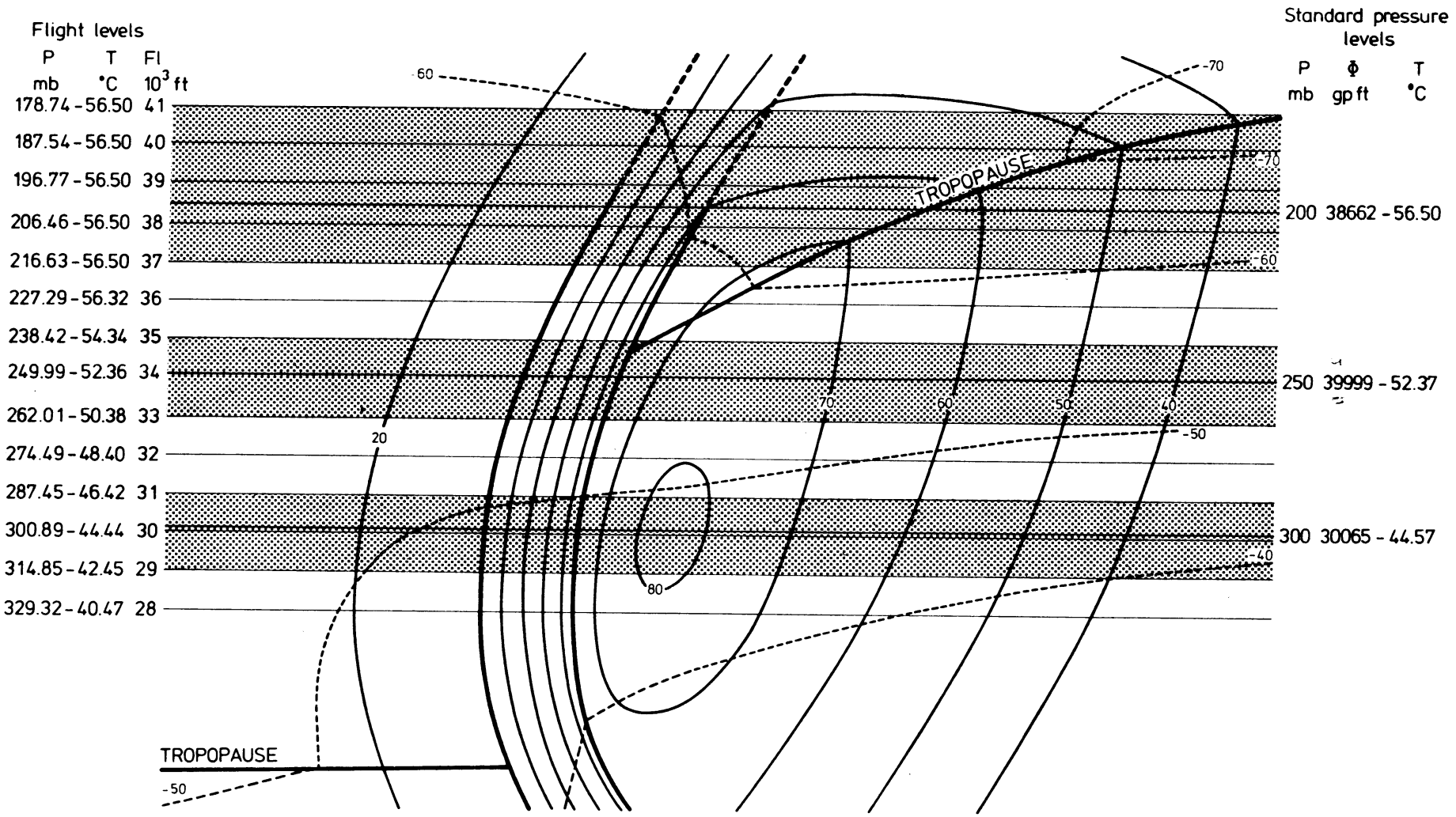

Figure 10 Cross section through polar front (schematically) in the airspace between 300 and 200 mbar.

(jet core). The interpolation of the data to the nearest standard pressure levels should therefore be handled with utmost care so as to avoid large interpolation errors.

In the model used in an experimental computer program we have selected the material in such a way that only those data points are retained that are within 1500 ft from the 300, 250 or 200 mbar level. (cf. the hatched bands in Fig. 10).

The flight levels selected for 300 mbar are Fl. 29, 30 and 31, for 250 mbar Fl. 33, 34 and 35, and for 200 mbar Fl. $\geqslant 37$. Only reports at Fl. 32, 36 and $\leqslant 28$ are rejected.

As described in section 1.1.2 the number of reports is highest at uneven flight levels over the North Atlantic. After selection of the reports the number of usable AIREPs is highest at 250 mbar and lowest at 300 mbar. The number of rejected reports at fl. 32, 36 and $\leqslant 28$ is small.

Interpolation of the aircraft geopotential

The aircraft geopotential Φ_A is interpolated to the nearest isobaric level using the hydrostatic equation in the form:

$$\Phi_S = \Phi_A + R\, T_A \ln \frac{p_A}{p_S} \qquad (2.3.2.1)$$

Here T_A is the reported temperature (static air temperature), p_A the pressure corresponding to the flight level in the ICAO standard atmosphere with the sub-scale set at 1013.25 mbar and p_S the standard pressure (300, 250 or 200 mbar). Substitution of the reported temperarure T_A instead of an (unknown) average temperature in the layer (p_A, p_S) introduces an interpolation error.

Table III

Interpolation error in the geopotential Φ introduced by an error of 1° C in the temperature per 1000 ft in the ICAO standard atmosphere.

300 mbar	$\pm$ 1.3 gpm
250 mbar	$\pm$ 1.35 gpm
200 mbar	$\pm$ 1.4 gpm

Taking into account that T_A may differ maximally 2^o C from an average temperature in a 1000 ft layer, the interpolation error is not more than $\pm$ 3 gpm/1000 ft, which is acceptable. The aircraft geopotential may still be interpolated when the aircraft location is 2000 ft above or below an isobaric surface.

Another approach is via the so-called D-value.
At the aircraft position by definition

$$D = \Phi_A - \Phi_P \qquad (2.3.2.2)$$

where Φ_P is the pressure altitude corresponding to the flight level in the ICAO standard atmosphere.

Under the assumption that $\frac{\partial D}{\partial \Phi} \simeq 0$ the interpolated geopotential in the standard pressure level becomes

$$\Phi = \Phi_{P_{stand}} + D \qquad (2.3.2.3)$$

where Φ_{stand} stands for the pressure altitude of the standard pressure level in the ICAO standard atmosphere.

Interpolation of the reported temperature

The interpolation of the (static air) temperature reported in AIREPs to 300, 250 or 200 mbar requires information on the vertical temperature profile. The use of some model temperature profile however may introduce interpolation errors of the order of 3 to 4^o C per 1000 ft, because the tropopause level is not known in advance.

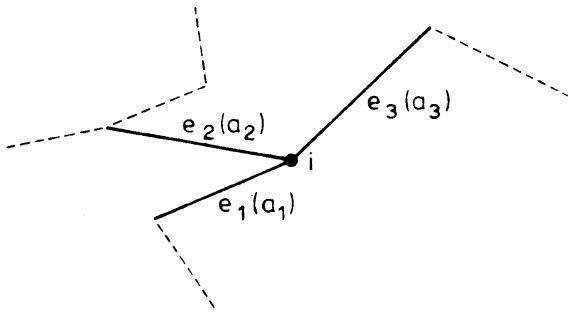

Fig. 11. Interpolation of the reported temperature in the tree structure.

In the experimental program we have applied the following procedure. Let the aircraft location be associated with the vertex i in the shortest spanning tree. (Fig. 11). Then search for all edges e_ρ (ρ= 1...m) incident with vertex i in the tree for which the endpoints

(a) are not on the same level;

(b) are not more than 2000 ft off the standard pressure level.

Find the isobaric temperature T_ρ by linear interpolation along the edge e_ρ using the reported temperature in the endpoints. Finally, form an average of T_ρ by using the weighted mean:

$$T \simeq \frac{\sum_{(e_\rho)} \frac{1}{(a_\rho)^l} T_\rho}{\sum_{(e_\rho)} \frac{1}{(a_\rho)^l}} \qquad (2.3.2.4)$$

where a_ρ denotes the length of the edge e_ρ and l is some suitable exponent. When m = 1, the temperature is maintained as reported and flagged.

Interpolation of wind data

In view of the lack of reliable information on the horizontal and vertical wind shear to be derived from data observed at different platforms (aircraft) the wind information is maintained as reported.

2.4 Quality control

The data handling in the aircraft reporting system includes many provisions for the making, recording and reporting of the observations, their air-to-ground transmission, their relay to MET stations and their distribution over the meteorological telecommunication channels.

Since so many actions are involved between the moment that a crew member reads the dials and the moment that the reports

arrive at destination, it is inevitable that the reporting system suffers from various error sources. In fact gross errors are not seldom in AIREPs. They are believed to be mainly administrative of nature. Probably we have to await the development and operational use of automatic data links before a drastic improvement in the quality of these reports may be anticipated.

Needless to say that quality control of these reports is of vital importance. Especially in the case of an application of combined processing to acquire aircraft geopotential values in a system mix, gross errors in the elements may render the processing valueless in the vicinity of an erroneous observation.

The checking of the content of the aircraft reports should start right at the beginning of the report processing in the form of an internal quality control. This control consists mainly in testing the individual elements in relation to a certain control parameter or limit of tolerance of the element concerned. The checking in terms of limits of tolerance states only whether a value of an element is nonsensical or dubious. Passing on to the phase of pre-analysis processing an additional space quality control is desirable. This space or horizontal quality control is carried out to ascertain that the primary data fit well in with the data from adjacent data points.

2.4.1 Space quality control

To achieve an objective and quantitative space quality control a suitable numerical aid is sought to be applied in the geometric graph associated with the network of data points in the system mix.

It is clear from the outset that the geopotential theorem (2.2.8), when brought into a convenient form, might be useful for this purpose.

When we take a closed integration path, Eq. (2.2.8) becomes

$$\oint \frac{f}{m} (u_g \, dy - v_g \, dx) + \oint RT_v \, d\ln p = 0 \qquad (2.4.1.1)$$

This "circuit theorem" discloses an interrelationship between the geostrophic approximation and the hydrostatic equation. When we substitute for the measured wind and temperature and other parameters, the theorem holds only approximately. Therefore, if we put a limit of tolerance (δ) to the off-zero circuit integral value, then the integral constraint

$$\left| \oint \frac{f}{m} (u\, dy - v\, dx) + \oint RT\, d\ln p \right| \leqslant \delta \qquad (2.4.1.2)$$

might serve as a test of the consistency of the measured elements in an arbitrarily chosen circuit.

In the airspace covered by long-range air transport the choice of a proper limit δ is governed by various factors: extreme values of wind- en temperature gradients between 200 and 300 mbar, the magnitude of ageostrophic winds, temperature discontinuities (front, tropopause) and in particular by the scale of the area enclosed by the circuit. In expression (2.4.1.1) limits should be determined for both terms on the left. Estimates of the tolerance limits can best be derived from known climatological structure parameters of both wind and temperature profiles.

As an example we evaluate the circuit integral in a simple 3-points circuit (triangle). Let a (sloping) triangle be specified by the vertices (x_1,y_1,z_1), (x_2,y_2,z_2) and (x_3,y_3,z_3) in a local (xyz) coördinate system. (Fig. 12).

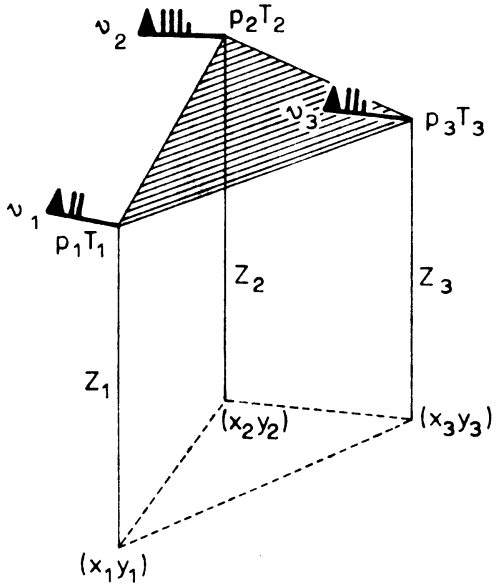

Fig. 12. Triangular check.

The data sets consist of pressure values p_1, p_2, p_3, temperatures T_1, T_2, T_3 and the wind velocities $(u_1, v_1, 0)$, $(u_2, v_2, 0)$ and $(u_3, v_3, 0)$.

Then, after some elementary calculation (cf. Eq.(2.2.10)), it is found that the integral constraint assumes the following linearized form:

$$\left(\frac{\bar{f}}{m}\right)\Big[\, y_1\,(u_3-u_2) + y_2\,(u_1-u_3) + y_3\,(u_2-u_1) + x_1\,(v_2-v_3) + x_2\,(v_3-v_1) + x_3\,(v_1-v_2)\Big] + R\left[T_1 \ln\frac{p_2}{p_3} + T_2 \ln\frac{p_3}{p_1} + T_3 \ln\frac{p_1}{p_2}\right] \simeq 0 \qquad (2.4.1.3)$$

R is the gas constant for dry air.

2.4.1.1 Some specializations

(a) In an isobaric surface, p = const., Eq.(2.4.1.1) becomes

$$\oint \frac{f}{m}\,(u\,dy - v\,dx) \simeq 0 \qquad (2.4.1.1.1)$$

This dynamical constraint is known to govern the horizontal consistency test for isobaric winds.

Note: If reference is made to the well-known theorem of Gausz or Green in two dimensions in a (xyp) coördinate system, then the vanishing of the closed line integral states that the wind is quasi non-divergent (div $\vec{v} \simeq 0$) in the area enclosed by the circuit.

In practice this consistency test is usually worked out in a 3-points circuit. Eq. (2.4.1.3) then becomes:

$$y_1\,(u_3-u_2) + y_2\,(u_1-u_3) + y_3\,(u_2-u_1) + x_1\,(v_2-v_3) + x_2\,(v_3-v_1) + x_3\,(v_1-v_2) \simeq 0 \qquad (2.4.1.1.2)$$

It deserves mentioning that when using this horizontal consistency test we are not able to detect temperature errors.

(b) When the circuit "degenerates" into a chain along the vertical axis traversed in both directions, we obtain

$$\oint R\, T_v \, d\ln p \simeq 0 \qquad (2.4.1.1.3)$$

This closed line integral describes the well-known hydrostatic check, which is commonly used in the internal quality control of upper air code reports.

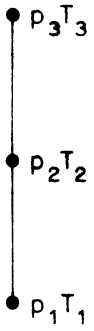

Fig. 13. Hydrostatic check.

In a 3-points chain (Fig. 13) Eq. (2.4.1.3) becomes

$$T_1 \ln \frac{p_2}{p_3} + T_2 \ln \frac{p_3}{p_1} + T_3 \ln \frac{p_1}{p_2} \simeq 0 \qquad (2.4.1.1.4)$$

It is noticed in passing that this hydrostatic check is not appropriate to discover errors in the wind velocity.

(c) The 3-points circuit constraint (Eq. (2.4.1.3) admits another interesting application in a system mix when a radiosonde station is bypassed by an aircraft at a close distance. (Fig. 14). If we suppose that the radicsonde

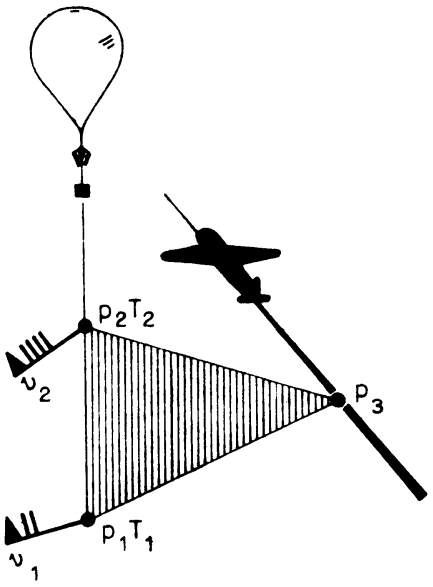

Fig. 14. Temperature check.

station functions as a calibration station, then we are able to compute the temperature at the aircraft location as follows:

Let the vertices of a triangle consist of the aircraft reporting point and two consecutive significant points of the upper air sounding which are closest to the aircraft position. Further, let (T_1,v_1,p_1) and (T_2,v_2,p_2) be the upper air data associated with these significant points. Then, with $p_1 \geqslant p_3 \geqslant p_2$ and $x_1 = x_2$, $y_1 = y_2$ Eq. (2.4.1.3) yields:

$$R\, T_3 \ln \frac{p_1}{p_2} = R \left[T_1 \ln \frac{p_3}{p_2} + T_2 \ln \frac{p_1}{p_3} \right]$$

$$+ (x_3-x_1)(v_2-v_1) + (y_3-y_1)(u_1-u_2) \qquad (2.4.1.1.5)$$

Given the pressure altitude of the flight this expression allows to calculate a temperature value at the aircraft position using only radiosonde data. This computed value may then be compared with the reported aircraft temperature, so that this quality control opens

the way to detect and eventually correct erroneous aircraft temperature data. It can be shown by the way that the above expression Eq. (2.4.1.1.5) is an immediate consequence of a special interpretation of the thermal wind equation applied to the wind- and temperature profiles of the sounding.

2.4.1.2 Application

In the space quality control of aircraft reports the circuit theorem should be used in its primitive form (2.4.1.1), because the aircraft locations are in general distributed at random in space.

In the geometric graph this means that the theorem should hold approximately in each circuit of the graph or at least in a set of independent circuits constituting a circuit basis. The reference to a circuit basis is a consequence of a graph theorem stating that the vanishing of the circuit integral along each independent circuit of a circuit basis automatically entails its vanishing along all possible circuits of the graph.

If the off-zero value of the line integral in one such circuit exceeds the preset limit of tolerance δ, this is an indication of the presence of erroneous data somewhere in the circuit, but it is impossible to pin-point the exact location(s) of these erroneous data. Moreover, if the precise location would be known, the theorem would not reveal whether the error is to be found in the temperature, the wind or in the position coördinates (latitude, longitude, pressure altitude). By cross-checking the values of circuit integrals the search for the precise localization of the erroneous data may be narrowed down, but still without the security of a precise localization. This finding clearly expresses that the use of the circuit theorem as an aid in space quality control has serious limitations.

However, we might also follow a more problem-oriented approach, for example by attempting to safeguard a reliable geopotential computation in the graph rather than detect and

eliminate or correct erroneous data. The method to be described below is based on the principle to remove "suspicious" edges and data points from the graph, which might otherwise adversely affect the accuracy of the computed geopotential values in the shortest spanning tree.

Triangulation check

The space quality control based on the circuit theorem seems to be most efficient when the set of circuits is scaled down to that of 3-points circuits or triangles, because within a "suspicious" triangle the data need to be rechecked in three points only. In a complete triangulation check involving all triangles in the graph, it is possible to discover some, if not all erroneous data points in a systematic manner. If the values of the circuit integral in all triangles, which are incident with one and the same vertex, exceed the tolerance limit, then it is most likely that the vertex is associated with an erroneous data point. Rather than recheck the measured or reported data, it is proposed to remove the suspicious edges. This may cause also the elimination of suspicious data points. The method consists of a systematic search for all triangles in the graphs accompanied by the evaluation of the circuit theorem in each triangle. Then the edges of triangles in which the circuit integral remains below the tolerance limit are retained in the graph; all others are expelled from the graph. It may then be anticipated that all edges incident with an erroneous data point will be expelled entailing the elimination of the erroneous data point itself.

This approach has been tried out experimentally. The method proved to be succesful when exercising some reasonable precautions. One of the precautions is connected with the phenomenon that in the triangulation check the specializations (a) and (b) of section 2.4.1.1 may appear. In case (a) the circuit integral fails to detect temperature errors, in case (b) the circuit integral likewise fails to detect wind errors. As a consequence, not all triangles incident with a vertex to be expelled from the graph need to be suspicious.

A second precaution deals with the edges which are not covered by the triangulation check. These have to be retained in the graph. It is acknowledged that this somewhat heuristic approach admits a variety of competative methods. The proposed method is easily executable on a computer, primarily because the total number of triangles to be searched is not excessively high.

2.5 Pre-analysis processing of SIRS data in the system mix

The pre-analysis processing of aircraft data in the system mix of radiosonde, aircraft and satellite observations should be followed by the updating of SIRS data to standard isobaric surfaces.

Referring to table II we observe that SIRS reports comprise temperature data for 15 standard levels and the geopotential thickness values for 14 layers relative to 1000 mbar. To derive the absolute geopotential from the thickness values we need some reference value at the SIRS position. This reference value may be inferred from an analyzed geopotential chart or may be derived from geopotential information available at nearby data sources.

In the present system mix it is plausible to take the data points of aircraft- and/or radiosonde observations as tropospheric reference points for updating the SIRS information.

First a selection is made from the available SIRS material of those reports that are valid in the principal time interval centred about the main synoptic hour. Then the updating of SIRS geopotential information proceeds as follows:

1. A reference geopotential at the SIRS position is derived from the geopotential of a nearby radiosonde- or aircraft data point, "nearby" specified in terms of a certain area of influence. The area of influence is assumed to be elliptical with the major axis in the direction of the wind. (Fig. 15).

$$r \leqslant \frac{a}{2}(1 + |\alpha|)$$

$$\alpha = \frac{\vec{r} \cdot \vec{v}}{rv} \qquad (2.5.1)$$

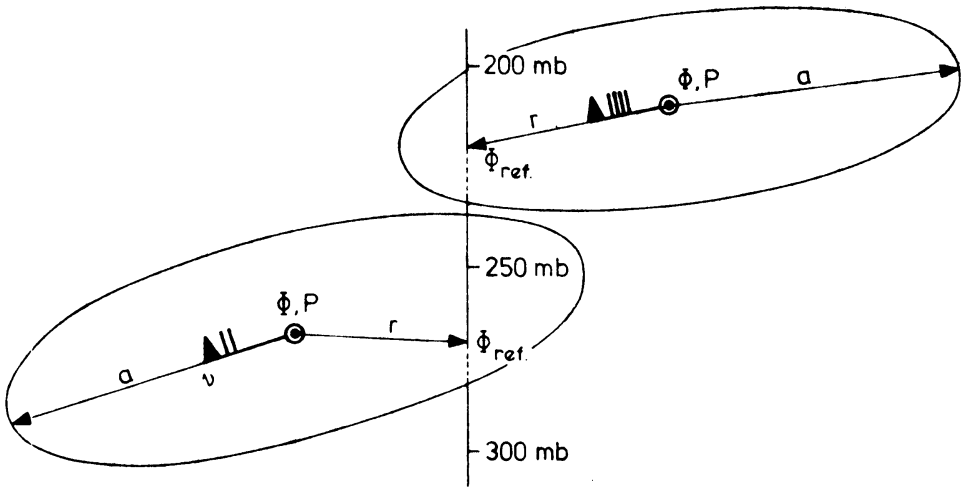

Fig. 15. Updating of SIRS geopotential data using processed aircraft data as a reference.

Here, $\vec{r}$ $(\Delta x, \Delta y)$ is the position vector of the SIRS position relative to a data point. $\vec{v}$ (u,v) is the wind velocity and a is a preset maximum range of influence in the wind direction.

2. An estimate of the reference geopotential at the SIRS position may be obtained by calculating the gradient of height geostrophically from the reported wind:

$$\Phi_{ref.} = \Phi + \frac{f}{m} (u \, \Delta y - v \, \Delta x) \qquad (2.5.2)$$

where Φ is the "aircraft" or "radiosonde" geopotential.

3. The reference geopotential in the SIRS position is valid at a pressure level P equal to that reported in a radiosonde data point or corresponding to the reported pressure altitude of an aircraft data point. Using the geopotential thickness values submitted by the SIRS reports:

$$D_1 = \Phi_{200} - \Phi_{1000}$$

$$D_2 = \Phi_{250} - \Phi_{1000}$$

$$D_3 = \Phi_{300} - \Phi_{1000}$$

we may deduce from this reference value an estimate of the SIRS geopotential at 250 mbar:

$$\Phi_{250} = \Phi_{ref.} + \frac{\ln P - \ln 250}{\ln 250 - \ln 200} (D_1 - D_2), \quad P \leqslant 250$$

$$\text{or} \quad \Phi_{250} = \Phi_{ref.} + \frac{\ln P - \ln 250}{\ln 300 - \ln 250} (D_2 - D_3), \quad P > 250 \qquad (2.5.3)$$

4. The best approximation of Φ_{250} may be a linear combination of the various estimates of all nearby data points as follows:

$$\Phi_{250} = \sum_i \frac{g_i \, \Phi_{250,i}}{\sum_i g_i} \qquad (2.5.4)$$

where the g_i are weight factors. In conformity with the previously used expressions for a spatial averaging we put:

$$g_i \sim \frac{1}{a_i} \ ,$$

where a_i stands for some distance measure. To ensure that a higher weight is given to estimates originating from data points which are up- or downstream rather than abeam of the SIRS position, a_i is defined as:

$$a_i = r + \left| \frac{\vec{r} \cdot (\vec{v} \times \vec{k})}{v} \right| \qquad (2.5.5)$$

In this way we come in the possession of additional 250 mbar geopotential data at the SIRS positions.

5. The corresponding geopotentials which are valid at the remaining 14 standard pressure levels are easily derivable using the reported thickness values D_1, D_2,....

e.g.
$$\Phi_{1000} = \Phi_{250} - D_2$$
$$\Phi_{300} = \Phi_{250} - (D_2 - D_3)$$
$$\Phi_{200} = \Phi_{250} - (D_2 - D_1) \qquad (2.5.6)$$
etc.

Together with the reported isobaric temperature these satellite geopotential data form a valuable additional data set to be used in the preparation of charts or in models of numerical analysis and prediction.

2.6 Experimentation

In this section we describe a numerical experiment which was arranged to exploit the feasibility of the method of combined processing in the system mix of upper air observations covering the North Atlantic airspace. The set-up of the experiment is indicated in the block-scheme below.

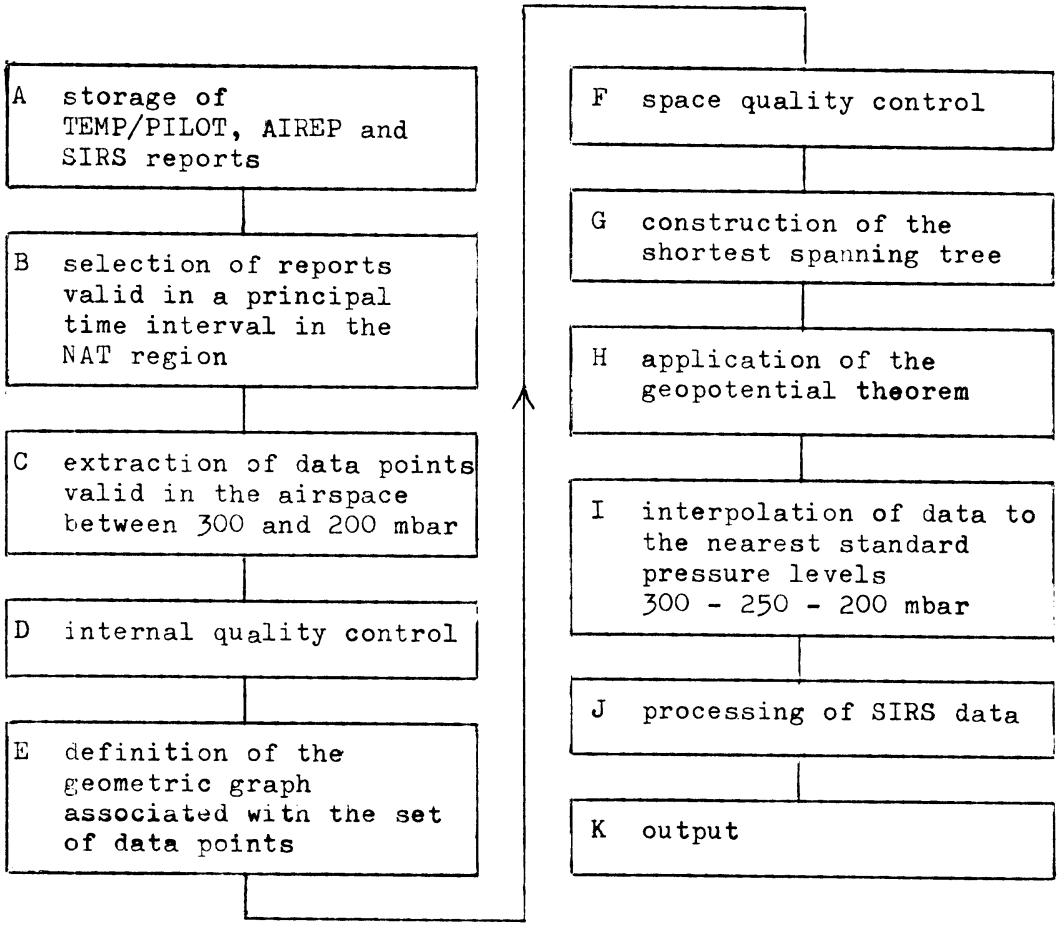

The blocks A, B, C and D describe the main features of the report processing procedure. The remaining blocks deal with the problem of pre-analysis processing.

Some comments

ad B A relatively broad time interval is needed to ensure the collection of sufficient aircraft reports and satellite reports (6 to 8 hrs) around the main synoptic hours.

ad C In the selection of radiosonde observations it is possible to select more than one data point for a single upper air sounding. The data points may refer to standard pressure levels but also to significant levels (tropopause, maximum wind).

It may happen that in the principal time interval different aircraft report at the same position. This gives rise to multiple data points, which introduce loops in the corresponding vertices of the geometric graph.

ad E In the geometric graph associated with the sets of data points of aircraft and radiosonde observations a pair of vertices is connected by an edge if the spacing of the data points remains below a preset limit. In view of the aircraft reporting procedures a wider spacing need to be specified in the E-W direction than in the N-S direction. Since the combined processing will be carried out in the shortest spanning tree, which consists of the smallest edges in the graph, the choice of a maximum spacing is not critical. Edges which connect data points of radiosonde stations may be removed from the graph. The graph is a spatial graph including vertical edges and even edges of zero length in case of multiple data points.

ad F The space quality control is based on the triangular check as explained in section 2.4.1.2. Let a_i, b_i, $i = 1,2,3$ denote the length (km) of the horizontal and vertical projection respectively of the edges of a triangle. Then we put for the tolerance limit δ in the dynamical constraint (2.4.1.2) (δ in gpm):

$$\delta = 0.05\, a + 10\, b,$$

where $a = \max_i a_i$

$b = \max_i b_i$

The effect of this triangular check is the removal of some vertices and/or edges from the graph structure, which would cause dubious errors in the path integration of Eq. (2.2.8).

ad G The construction of the shortest spanning tree is based on the method of Dijkstra. See section 2.3.1.3. Actually, use is made of a computer algorithm developed by Whitney [15]. This algorithm also covers the construction of a shortest spanning forest when the geometric graph is disconnected.

ad H The calculation of the geopotential runs parallel with the construction of the shortest spanning tree as explained in section 2.3.1.3. Afterwards the computed geopotential values are matched with those reported in the data sets of radiosonde stations using formula (2.3.1.3.1) and they are subsequently corrected according to the formula (2.3.1.3.2) where a_j denotes the Cartesian distance between a vertex and a radiosonde data point and where $l = 2$.

ad I Based on the reported pressure altitude the enlarged data sets of aircraft reports are divided into three groups appertaining to the 200, 250 and 300 mbar levels. The meteorological data are interpolated to these levels according to the instructions given in section 2.3.2. The selection procedure may cause some aircraft data to be exempted from further processing.

ad J The updating of SIRS is performed according to the scheme proposed in section 2.5. If a satellite observation is out of the range of influence of all aircraft and radiosonde data points, then only the temperature parameter of the SIRS report remains useful.

Before discussing some experimental results it is pointed out that at the time of writing this report there has not been made a start yet with the automation of the report processing, which means that only a few trials could be made.

Results

Fig. 16 shows in perspective the structure of a (spatial) shortest spanning tree for 4 June 1974, 00 GMT ± 4 h. The tree vertices refer to data points of aircraft and radiosonde stations. Included are aircraft positions for reports in continental airways, which were obtained from some series of post-flight reports. The tree structure is typical of the North Atlantic Region. It is observed that the main branches run north to south along the reporting meridians. Note also the vertical branches where aircraft observations happen to be stacked in the vertical at the same geographical positions and where the branches form part of the balloon track of upper air soundings. Some radiosonde data points are isolated from the main tree. They form separate tree components, because the spacing of these data points to the vertices of the main tree is too large. Strictly speaking these tree components constitute a shortest spanning forest.

From a point of view of combined processing this tree structure is not very efficient. The tree should have a more rugged appearance, which means that the horizontal distribution of the aircraft reporting points needs to be more homogeneous and isotropic. To improve the distribution of the reporting points it would be required to review the existing air reporting procedures.

The result of a combined processing experiment is shown in Fig. 17. The figure displays the hand-drawn contours in a 250 mbar chart for 7 January 1975, 12 GMT ± 4 h. The chart was prepared using the output of an experimental computer program developed to apply the method of pre-processing as outlined in this report.

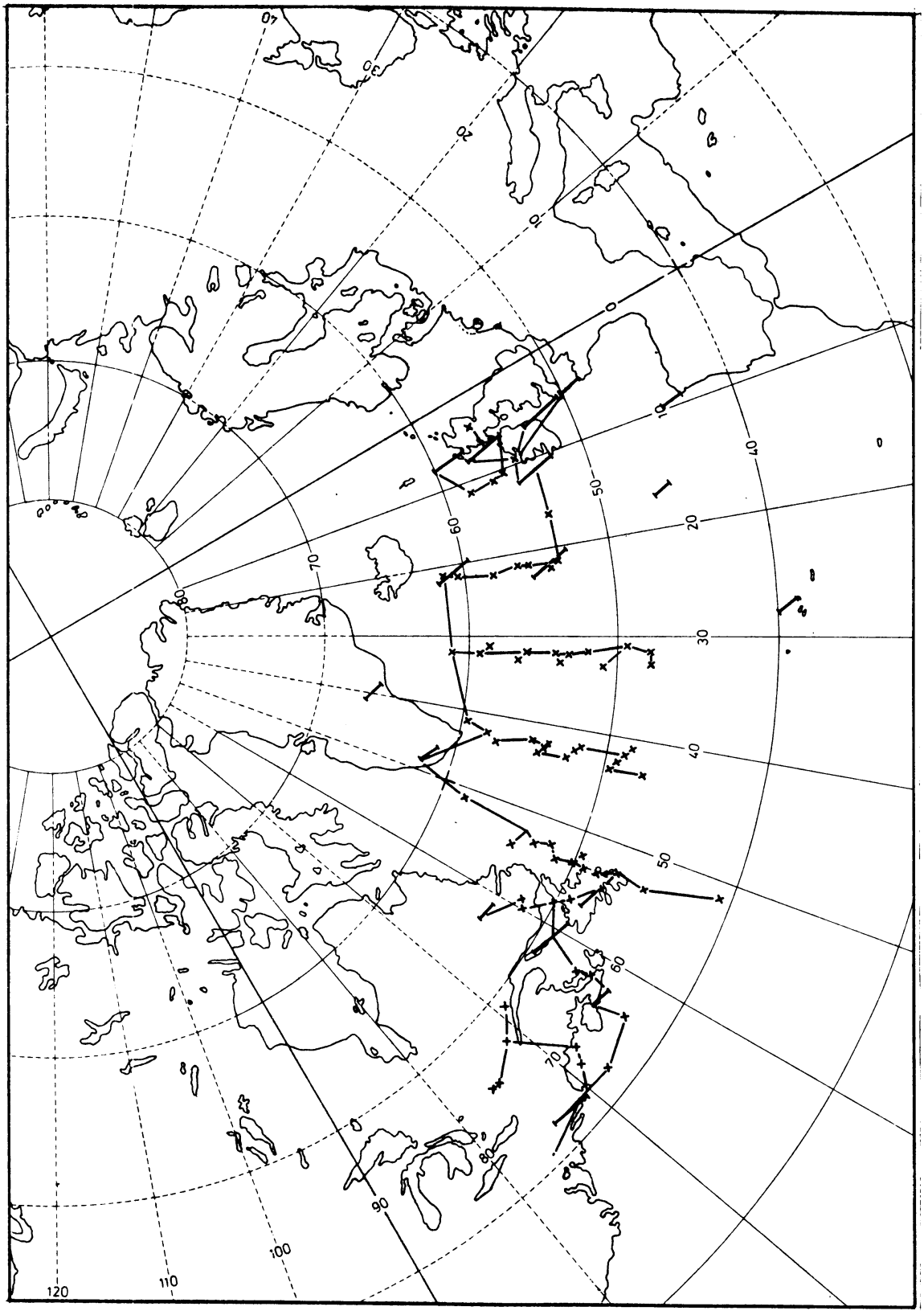

Figure 16 Spatial shortest spanning tree (forest) in perspective through radiosonde- and aircraft data points.
4 June 1974, 00 GMT ± 4 hours.

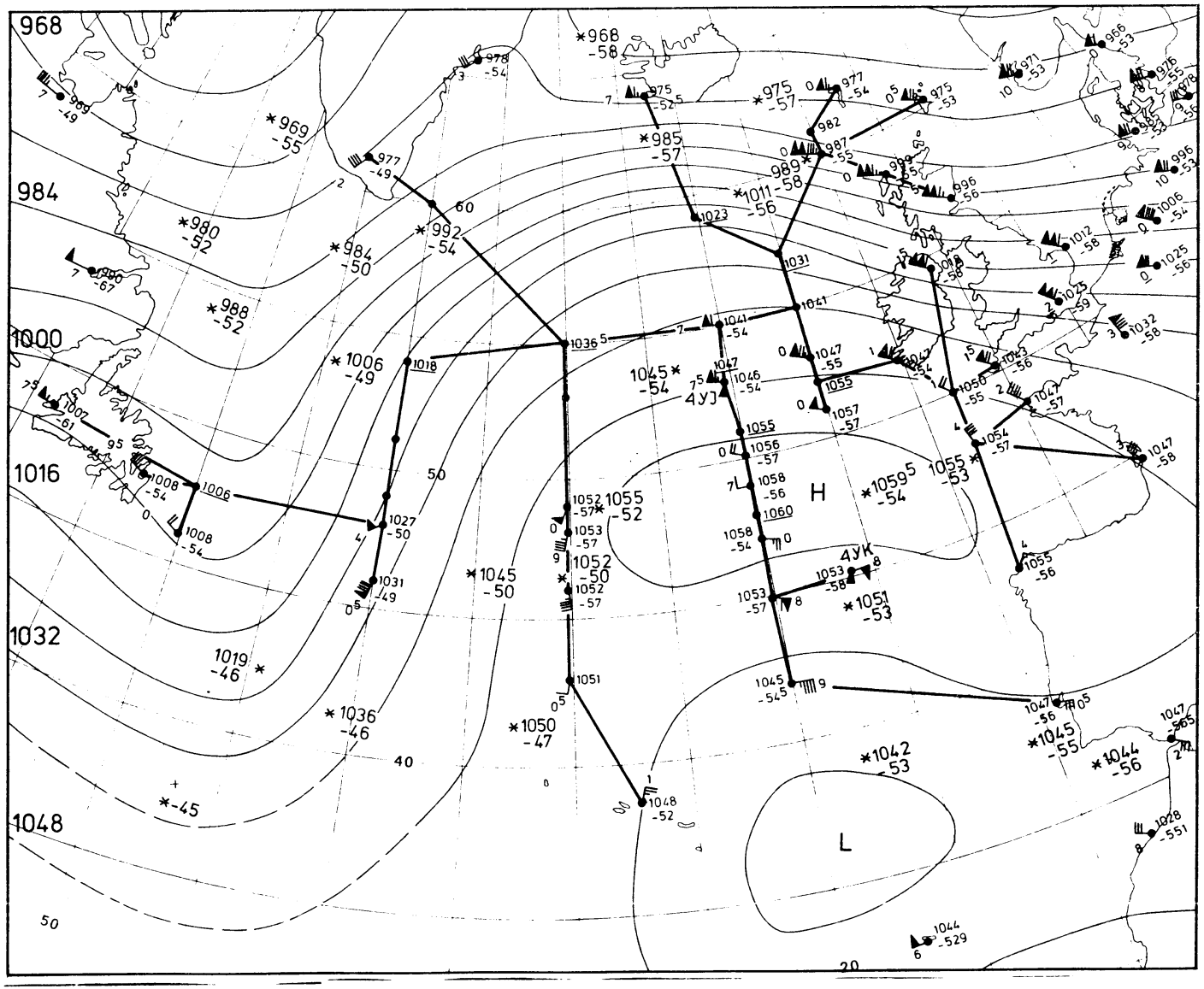

Figure 17 250 mbar contour analysis for 7 January 1975, 12 GMT ± 4 hours, based on radiosonde/rawin and computer-processed aircraft and satellite data. The data points are connected by a shortest spanning tree. For further details see text.

The network of data points is the same as depicted in Fig. 7, with some additional data from continental upper air stations. The plottings refer to the following data points:

(a) Φ , T and $\vec{v}$, radiosonde observations;

(b1) Φ , T and $\vec{v}$, processed aircraft observations at Fl. 33, 34 and 35;

(b2) Φ , underlined, processed aircraft observations at Fl. 32 and 36;

Note: In case the reports refer to the same geographical position, e.g. 46 N, 30 W, the data have been averaged;

(c1) Φ and T, processed satellite observations;

(c2) T, for satellite observations which are outside the area of influence of nearby aircraft and radiosonde observations (e.g. at position 32.4 N, 47 W).

Over the North Atlantic only two ocean station vessels (4YJ and 4YK) were available to act as calibration stations. The number of aircraft observations is highest in the eastern part of the Atlantic, in accordance with the observational characteristics as described in section 1.1.2. SIRS positions are indicated by an asterisk.

The figure also depicts the (horizontal projection of the) shortest spanning tree along which the geopotential formula (2.2.8) has been applied. All vertices incident with the tree are indicated including those related to aircraft positions which are not selected for interpolation of the data to the 250 mbar level (e.g. position 53 N, 30 W). It might appear that some edges, e.g. the edge connecting the positions 55 N, 30 W and 60 N, 40 W, should not be a branch in this shortest spanning tree, because other edges like the one connecting the positions 54 N, 40 W and 60 N, 40 W are shorter. The reason for this is that these shorter edges had been expelled from the graph during the process of space quality control (triangulation check).

The horizontal consistency of the data warrants an uncomplicated smooth drawing of the contour lines especially where the data are plentiful. The same applies, but to a lesser extent, to the drawing of isotherms.

Verification

It is of vital importance to have an impression of the accuracy attainable in the analysis of the parameter fields using data from a pre-analysis processing in the system mix. The verification of the analysis is difficult, simply because we lack sufficient independent observational material to compare the analyzed values with those observed.

We can arrange for simulation experiments in which some data points of upper air soundings are withhold from the combined processing, in order to be used as test material. In data-sparse areas, however, the removal of such information would adversely affect the accuracy of the processing, and this would render the verification virtually worthless. Simulation experiments can also be planned over continents with a dense network of upper air observations. In a dense network of a size comparable with that covered by the transatlantic crossings we may simulate the system mix by taking away a set of these upper air data from the network and let them figure as aircraft reports. The same data are used afterwards to check the performance of the combined processing carried out in the artificial network.

A few such experiments performed over the North American continent have revealed that the analysis error between 200 and 300 mbar is of the order of the RMS error of radiosonde observations.

2.7 Use in numerical prediction models

In what follows a few comments are made on the usefulness of the processed data in a system mix in models of numerical analysis and prediction.

1. In general objective analysis the initial field of a meteorological parameter is defined in the points of a regular grid. The grid point values are derived from the quasi-randomly distributed data points utilizing a proper interpolation scheme.

   Especially in primitive equation models the initial field data need to be satisfatorily balanced, because inbalances between pressure and Coriolis-forces can lead to large-amplitude inertial gravity waves. This problem of initialization is the subject of numerous investigations [5].

   Various approaches to the solution of the problem have resulted in the development of suitable procedures in static initialization, dynamical initialization and initialization by statistical methods.

   As to the static initialization, there is a general trend now to start the computation directly from the analysis if the mass field and wind field are coupled during the analysis by dynamical constraints.

   When the pre-processed data delivered by the observations in a system mix are used in objective analysis, it is believed that the method of combined processing fits well with this trend in static initialization, because the processing is governed by coupling the mass field and wind field using the geopotential theorem as a dynamical constraint.

2. The method of combined processing operates on observational material, which is valid in the principal time intervals around 00 and 12 GMT. As a special feature the processing method also introduces some time averaging, so that the processed data even tend to become quasi-synoptic. Operationally this means that the data supply in the system mix matches with the current schemes of numerical analysis-prediction models.

   When the processed data in a system mix serve as input in such models, a large proportion of aircraft data, notably those valid in-between the principal time intervals, is not

assimilated at all, which means that valuable information is lost.

The use of all asynoptic data in meteorological data processing requires the insertion of these data in schemes of 4-dimensional data assimilation. In such 4-dimensional assimilation models the data may be inserted quasi-continuously, but then there is a risk that shocks are produced, because the data are in general not compatible with the prediction model. The data may also be assimilated intermittently, which means that the data assimilation takes place at separate times. Then the asynoptic data need to be sampled in groups within appropriate time intervals. In this context it is interesting to investigate whether by some extension of the combined processing method the 4-dimensional data assimilation meets with success, in particular whether shocks and breaks may partly or wholly be suppressed.

The proposed modification of the method is based on the principle that not only radiosonde data points may act as reference values but processed aircraft data as well. Suppose that the available data in the system mix have been sorted in terms of the reported observation times. Then we may distribute this sorted material over a set of consecutive and partly overlapping time intervals. (Fig. 18). It is the intention to apply the combined processing method in each interval i. Then the process is continued in time interval i+1 using the processed aircraft data in the overlap with the previous interval i as reference values. In order that this processing be successful it is required that there are sufficient reference data to be processed in each interval. Therefore the intervals and the overlaps on the time axis should be of variable length, dependent on the rate of supply of data.

Note: Before the processing proceeds the data in a given time interval may first be interpolated to the central time, e.g. by using an advection method.

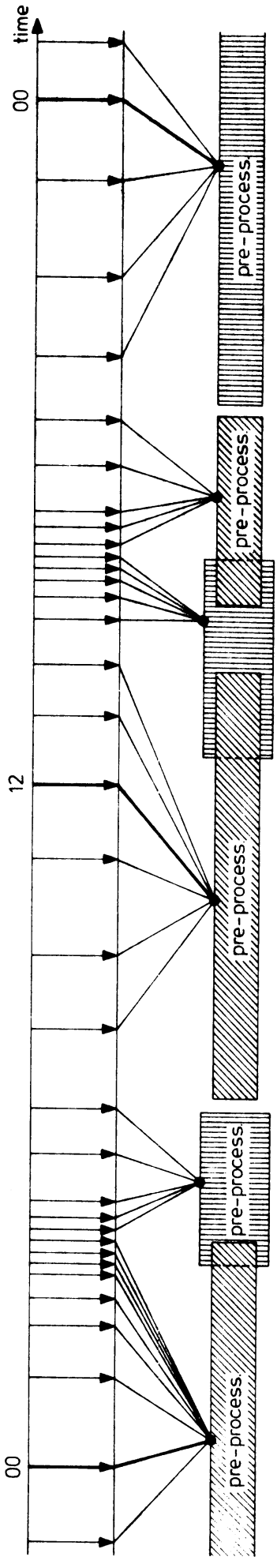

Figure 18 Scheme of combined pre-processing in a system mix for the purpose of intermittent 4-dimensional data assimilation.

Because the provision of aircraft reports is known to be quite irregular in a 24-hours period, the interval length may range from 2 to 8 hours. If the data set in a time interval contains also radiosonde data points, it may occur that the time overlap need not be specified at all.

This scheme of combined processing in a system mix is thought to be suited for incorporation in some type of intermittent 4-dimensional data assimilation process, but its usefulness remains to be proved by further experimentation.

2.8 Individual flights

A series of consecutive aircraft observations of an individual flight is considered to have a better spatial consistency than separate observations reported by different aircraft. These observational series are also better suited to display the meso-scale atmospheric features encountered during the flight. In the report processing phase of the data handling such series may easily be extracted from the hourly collection of reports by searching for those reports that have the same aircraft identification and flight number.

These series of reports may be processed according to the principles laid down in section 2.2, provided that the series be complete. Series of post-flight reports suit this purpose, but series of in-flight reports are seldom complete, as in operational practice not all reports of an individual flight appear to be channelled through the GTS (cf. section 1.1.2). From a point of view of pre-processing the spacing of data points is marginal in view of the 10^{o} reporting procedure. Although modern equipment (INS, Doppler navigation) admits a higher rate of reporting, there are numerous restrictions which hamper the introduction of more stringent reporting schedules.

Extremely detailed meteorological information is obtainable now from the records of automatic data acquisition units. Wide-bodied aircraft equipped with these units sample environmental data at a rate of 0.6 s corresponding to an en-route resolution of $\pm$ 150 m.

2.8.1 Elimination of systematic errors

Some parameters in a series of observations such as wind and temperature will suffer from systematic errors due to maladjustments in the measuring equipment. These errors introduce bias into the reported values; they have no marked effect on the en-route gradients of the parameter. The problem to remove the observational bias is not easy to solve, because the detection and correction of systematic errors in wind and temperature require the availability of some independent and unbiassed control data as a reference. In a system mix the performance of a component system needs to be monitored by another system. The controlling system should of course be of a high quality. By way of example we shall describe a method to eliminate the possible temperature bias in a series of observations of an individual flight using the observational data of radiosonde stations as control data.

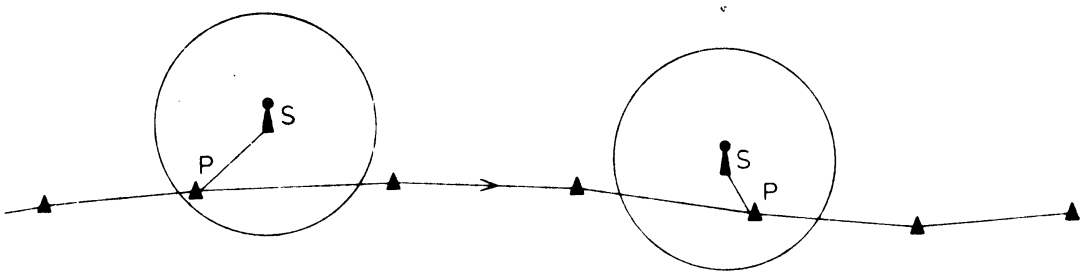

Fig. 19. Elimination of temperature bias in a series of aircraft reports of an individual flight.

First, the following assumptions are made. The temperature bias is considered to be constant along the en-route portion of the flight. At least one reporting point is in the proximity of a radiosonde station in time and space (up to 200 km, up to 3 hrs), and the accuracy of the radiosonde data is within tolerable limits (1 mbar, 1^{o} C, 5 m s^{-1}).

Now, let P be a reporting point in the vicinity of station S. (Fig. 19). Then, to obtain an estimate of the temperature at P,

we evaluate the circuit theorem in a special triangle as explained in case (c) of section 2.4.1.1. The departure from the reported temperature is interpreted as the temperature bias. Elimination of the bias in all reporting points yields a series of corrected temperatures along the flight track. The procedure may be repeated for as many points P and S meeting the above proximity conditions. The weight factors involved in the process of averaging may be specified in terms of the distance of approach of the points P and S and of the difference in observation times.

It is not feasible to develop a similar procedure for the removal of systematic wind errors, simply for the lack of a suitable diagnostic constraint to find an estimate of the wind velocity in the reporting point.

2.8.2 Geopotential computation using AIDS records

In section 2.2. it was pointed out that the geopotential computation could be performed for any individual flight, provided that the spacing of data points be not too coarse.

Aircraft equipped with AIDS units (airborne computer, data processing and magnetic tape storage) yield a wealth of en-route meteorological information, so much detailed that even small-scale phenomena may be analyzed. Observational series of these flights are particularly suited to be utilized for the path integration of Eq. (2.2.8). Fig. 20 shows the track of a flight with a DC-10 Amsterdam-Toronto. The plotted data were selected from a printed list of 1500 data points, climb and descent included. The diagrams show the temperature and wind profiles made during the ascent and descent portions of the flight. These profiles may be compared with the upper air soundings of De Bilt and Toronto, valid at the nearest 12 hours datum times.

Fig. 21 depicts the same flight in a 250 mbar chart valid for 2 August 1974, 12 GMT. The flight contains another series of data points including those that are related to significant features in the en-route wind and temperature profiles. Data

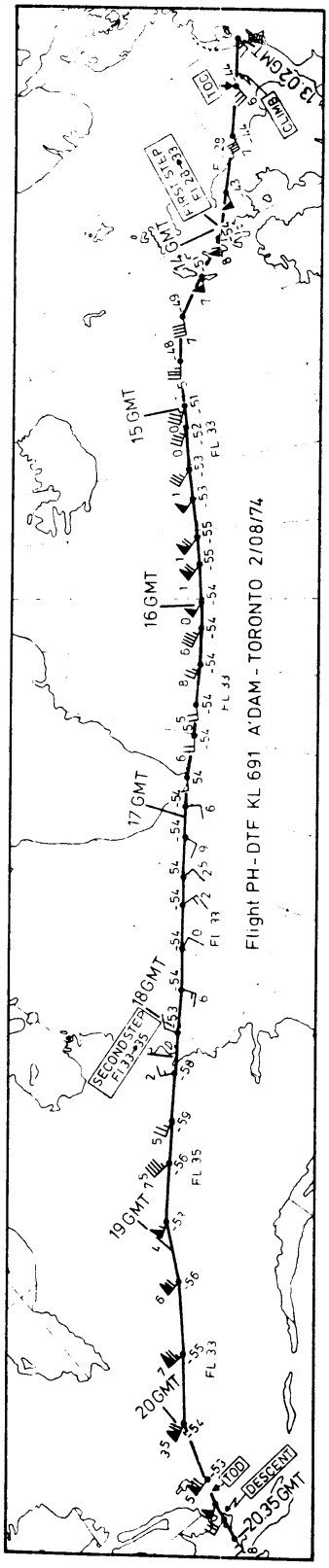

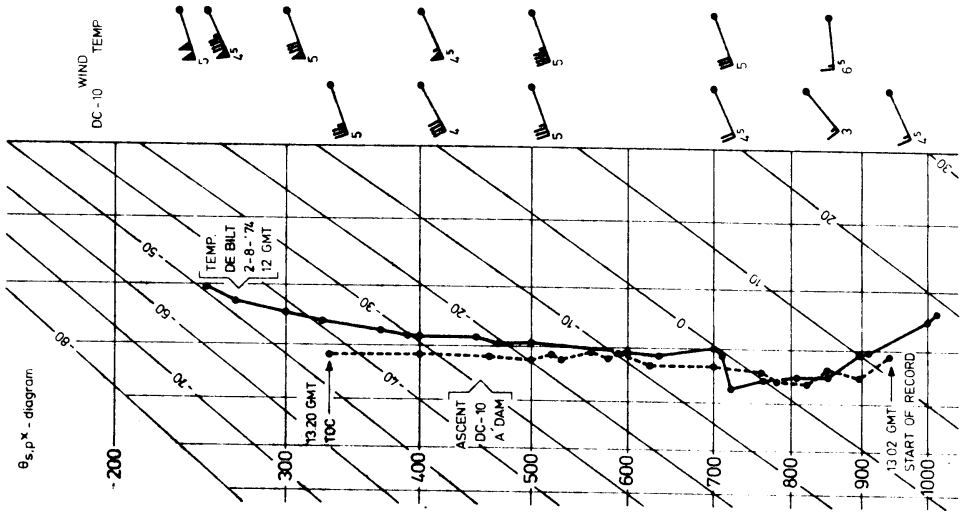

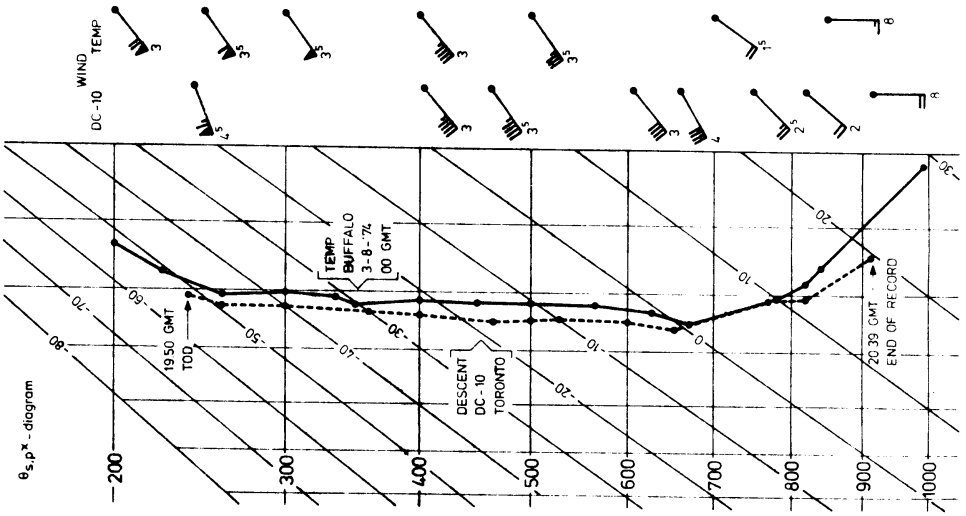

Figure 20 Flight of DC-10 equipped with AIDS unit, Amsterdam-Toronto, 1 August 1974, 13.02-20.39 GMT. Plottings refer to a highly compressed data set of wind and temperature retrieved from the tape record. The diagrams show the wind and temperature data for the climb and descent and for the upper air soundings of De Bilt (06260) and Buffalo (02528) valid at the nearest standard times. TOC = top of climb, TOD = top of descent.

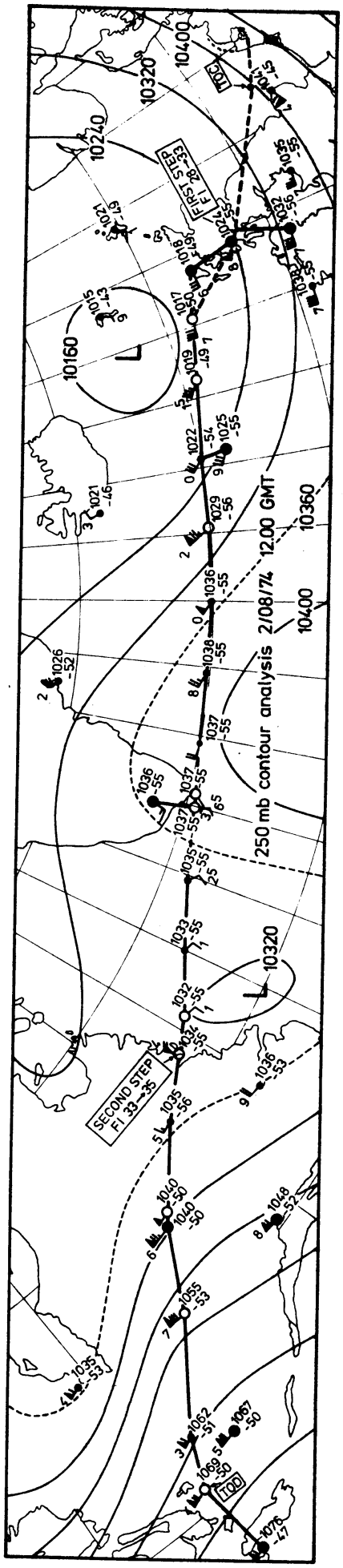

Figure 21 250 mbar chart valid for 2 August 1974, 12 GMT.
Same flight as depicted in Fig. 20. The en-route geopotential data were obtained by the application of the geopotential theorem and by interpolation. Heavy dots indicate the radiosonde stations, which were used as calibration stations.

points which refer to these atmospheric features are encircled.

Now, returning to the path integration the absolute geopotential associated with the AIDS data may be obtained using the same algorithms as developed for the integration of Eq. (2.2.8) in a shortest spanning tree. In the cruise portion of the flight the shortest spanning tree consists of the flight track sec except for some branches connecting the by-passed radiosonde stations and the nearest aircraft positions.

The absolute geopotential values submitted by the algorithm are matched with those reported for the radiosonde stations. They need afterwards to be interpolated to the nearest standard pressure level (250 mbar). In Fig. 21 the result of the path integration and interpolation is shown. The plotted values only refer to the portion of the flight between the first step and the top of descent (TOD). (Fl. 33, 35).

In the AIDS system the recording is also made in the ascent and descent phase of the flight. This opens the way to integrate the geopotential expression, starting right at the point of departure and continuing until the destination has been reached. Then the station height at the point of departure may be used as a datum to match the computed geopotential along the whole flight track. The radiosonde stations are rendered inoperative during the process. The processing then resembles the data processing of a single radiosonde observation with a comparable data resolution, but over a much longer path length.

The value of the computed absolute geopotential at the point of arrival should then match with the station height at the destination. Any departure from this station height is automatically compensated for by applying a suitable correction to the en-route geopotential data using formula (2.3.1.3.2). Departures of the computed geopotential from the station height at destination may be caused by various factors: observational bias, ageostrophic wind components, temporal change of the atmospheric circulation, etc. One of these factors is concerned with the substitution of the reported temperature for the adjusted virtual temperature in Eq. (2.2.8). The effect of

this substitution on the computed geopotential is negligible at cruising altitude, but in the ascent and descent portions of the flight this substitution may cause a bias in the computed geopotential of the order of 0.5 %. The overall effect on the computed geopotential at the point of arrival is small, because the bias in the ascent and descent partly compensate each other.

A numerical experiment elaborated for the Amsterdam-Toronto flight yielded a departure from the station height at Toronto of 5 gpm. At cruising altitude the geopotential was 3 to 4 gpdam too low compared with the geopotential taken from the 250 mbar analysis in Fig. 21.

2.9 Concluding remarks

We have seen that some well-known elementary dynamical and physical constraints could be amalgamated in the form of a suitable line integral theorem. The theorem has proved to be a useful numerical aid to derive additional geopotential information from the primary data conveyed by the various observational programmes in a system mix.

Moreover, when taking a closed integration path the theorem has also proved to be a suitable diagnostic tool for the purpose of space quality control of the reported data.

The feasibility of the method was demonstrated within the triad of observational systems of upper air data in the North Atlantic Region comprising radiosonde/rawin, aircraft- and satellite observations.

In future studies this system mix might be supplemented with observations of mobile ships, which are the main source of surface observations over the ocean. Surface pressure and temperature may for example be used as another datum for reference to update the geopotential information in the satellite reports. These add to the already available geopotential data of aircraft as tropospheric reference data for updating these SIRS data.

From an operational point of view the proposed method of combined pre-analysis processing has to await the development of suitable automatic data selection and extraction procedures from the material received over the international telecommunication channels. This aspect of report processing has so far been an obstacle to thoroughly exploring the feasibility of the method in practice. This also concerns the problem of quality control and the problem of integration in existing models of numerical weather analysis and prediction or models of 4-dimensional data assimilation.

We have also seen that the processing of meteorological material involved in the records of AIDS units offers the possibility of analyzing the state of the atmosphere with a resolution which is unprecedented in the past.

-o-o-o-

REFERENCES

1. WMO Technical Regulations, Vol. II and attachment A to chapter 12.

2. ICAO Annex 3 to ICAO Convention - Meteorology, chapter 3, attachment B in the PANS-MET and ICAO PANS-RAC, Part II and appendix 1.

3. WMO Technical Note No. 141, 1975. Utilization of Aircraft Meteorological Reports.

4. Bengtsson, L. and Morel, P., 1974. The performance of space observing systems for the first GARP Global Experiment. The GARP Programme on Numerical Experimentations, Report No. 6.

5. GARP Publication Series No. 15, 1975. 4-Dimensional Assimilation of Meteorological Observations.

6. de Jong, H.M., 1966. A new process for the Evaluation of Upper Winds. J. of Appl. Meteor., Vol. 5, pp. 436-449.

7. GATE report No. 11, 1974. Aircraft Plan for the GARP Atlantic Tropical Experiment, pp. 113-141.

8. de Jong, H.M., 1973. Example of Combined Processing and use of Information in a Hybrid System of Observations. Idöjárás, Vol. 77, pp. 265-269.

9. Berge, C., 1973. Graphes et Hypergraphes. Dunod, Paris.

10. Busacker, R.G., and Saaty, T.L., 1965. Finite Graphs and Networks. Mc Graw-Hill.

11. Roy, B., 1969-1970. Algèbre moderne et théorie des Graphes. Vol. 1 and 2.

12. Cayley, A., 1889. A Theorem on Trees. Quart. J. Math., Vol. 23, pp. 376-378.

13. Kruskal, J.B., 1956. On the shortest Spanning Subtree of a Graph. Proc. Am. Math. Soc., Vol. 71, pp. 48-50.

14. Dijkstra, E.W., 1959. A note on two problems in connection with graphs. Numer. Math., Vol. 1, pp. 269-271.

15. Whitney, V. Kevin. M., 1972. Algorithm 422. Minimal Spanning Tree. J. ACM. Vol. 15, pp. 273-274.

-o-o-o-

ANNEX

Observational requirements in the World Weather Watch Plan for 1976-1979

(a) Observational requirements for the global network for mid- and high latitudes

Temperature

Horizontal resolution	500 km
Vertical resolution	4 levels in troposphere
	3 levels in stratosphere
Accuracy	$\pm$ 1° C

Wind

Horizontal resolution	500 km
Vertical resolution	4 levels in troposphere
	3 levels in stratosphere
Accuracy	$\pm$ 3 m/s

Wind is ranked as lower priority than temperature, since it can be derived satisfactorily from temperature using balance relationships.

Relative humidity

Horizontal resolution	500 km
Vertical resolution	2 degrees of freedom in troposphere *)
Accuracy	$\pm$ 30%

Sea-surface temperature

Horizontal resolution	500 km
Accuracy	$\pm$ 1° C

---

*) Note: The humidity distribution in the vertical should be described by a tropospheric model profile having two independent parameters to be specified by observation.

ANNEX

Pressure

Horizontal resolution	500 km
Accuracy	± 0.3%

(b) Observational requirements for the global network from the tropics

Wind

Horizontal resolution	500 km over land
	1000 km over oceanic areas
Vertical resolution	4 levels in troposphere
	3 levels in stratosphere
Accuracy	± 2 m/s

Wind is considered a fundamental parameter in the tropics, because it is only weakly coupled to the mass field and cannot be satisfactorily derived from other parameters. Full vertical resolution is a critical requirement in the zone near the Equator.

Temperature

Horizontal resolution	same as wind
Vertical resolution	4 levels in troposphere
	3 levels in stratosphere
Accuracy	± 1° C

Relative humidity

Horizontal resolution	same as wind
Vertical resolution	2 degrees of freedom in troposphere
Accuracy	± 30%

Sea-surface temperature

Horizontal resolution	1000 km
Accuracy	± 1° C

ANNEX

(c) Data should be made available twice per day. Observations from conventional upper-air stations and surface stations should be made at the standard synoptic hours of 00 and 12 GMT. If local conditions dictate that observations be made at other times, these observations can be useful for the global network.

-o-o-o-

Tabel I

	datum	16/4	16/4	17/4	24/9	15/4/1975							23/9	27/10	gemiddeld ± standaard-afwijking	standaard-afwijking in het gemiddelde
	tijd / hoogte	07.52	06.20	18.00	00.08	13.09	13.23	13.35	13.53	14.04	14.11	14.16	11.27	15.00		
A	200 m	-0.2	1.1	0.3	0.2	0.4	-1.1	4.0	2.0	0.1	0	-2.3	-	-	0.4 ± 1.6	0.5
	160 m	-	-	0.8	0.9	-1.7	-0.5	1.9	1.7	-0.2	-0.7	-2.0	-	-	0.0 ± 1.4	0.5
	120 m	-	-	0.2	0.6	0.5	0	0.5	2.1	0.1	-0.6	-1.1	-	-0.4	0.2 ± 0.9	0.3
	80 m	-1.1	2.5	1.7	0.2	0.2	0.2	-0.7	3.4	0.7	0.5	0.5	0.4	1.4	0.8 ± 1.2	0.3
	40 m	-	-	1.2	-0.1	1.1	0.2	-1.2	2.8	0.7	0.1	-0.4	-0.7	-2.1	0.1 ± 1.3	0.4
	20 m	-	-	0.6	-0.3	0.4	0.4	-1.1	2.7	0.6	0.4	-0.8	1.8	2.5	0.7 ± 1.2	0.4
	10 m	-1.1	1.5	1.5	-0.5	-	-0.1	-1.3	-	0.5	0.3	-0.6	1.2	0	0.1 ± 1.0	0.3
B	200 m	5	-3	-1	4	3	18	25	32	23	19	4	-	-	12 ± 12	4
	80 m	8	12	7	1	-6	4	9	31	21	19	19	-	-	11 ± 10	3
	10 m	10	3	10	3	-	1	-9	-	27	21	21	-	-	10 ± 12	4

A : Verschillen tussen de gemiddelde windsnelheden te Cabauw en de AIDS-windsnelheden in m/s.

B : Verschillen tussen de gemiddelde windrichtingen te Cabauw en de AIDS-windrichtingen in graden.

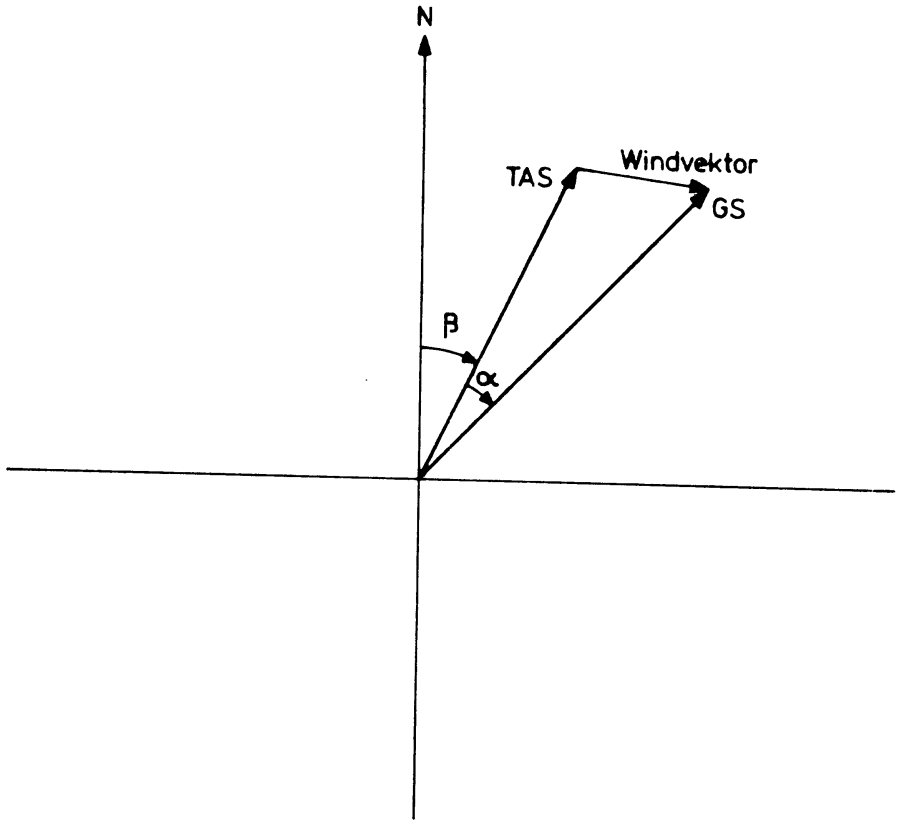

TAS = True airspeed
GS = Groundspeed
α = Drift angle
β = True heading

Fig. 1 Vektordiagram ter bepaling van de windsnelheid en windrichting.

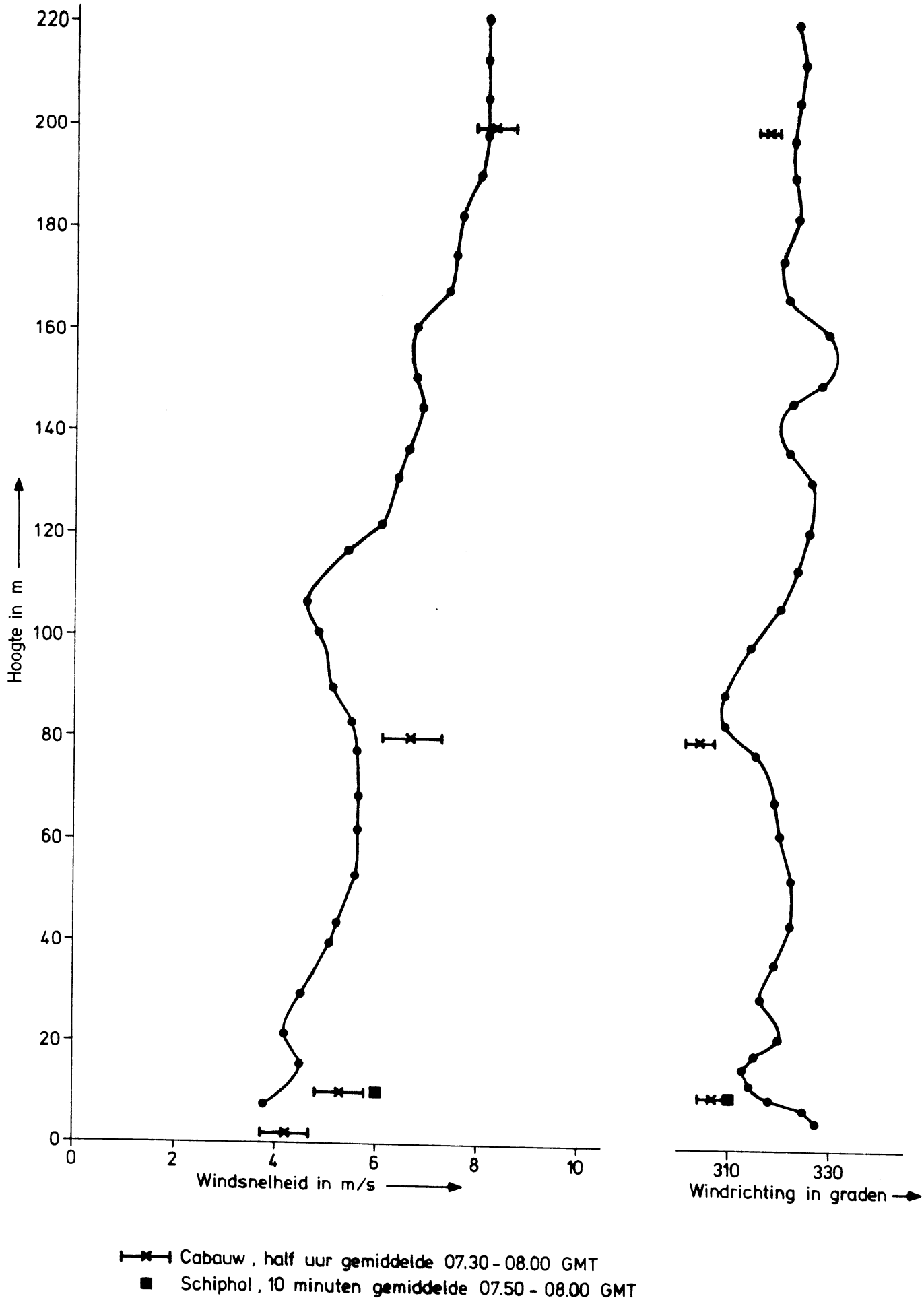

Fig. 2 Windsnelheid en windrichting gemeten tijdens een daling op 16-4-1975 om 07.52 GMT (touch-down tijd).

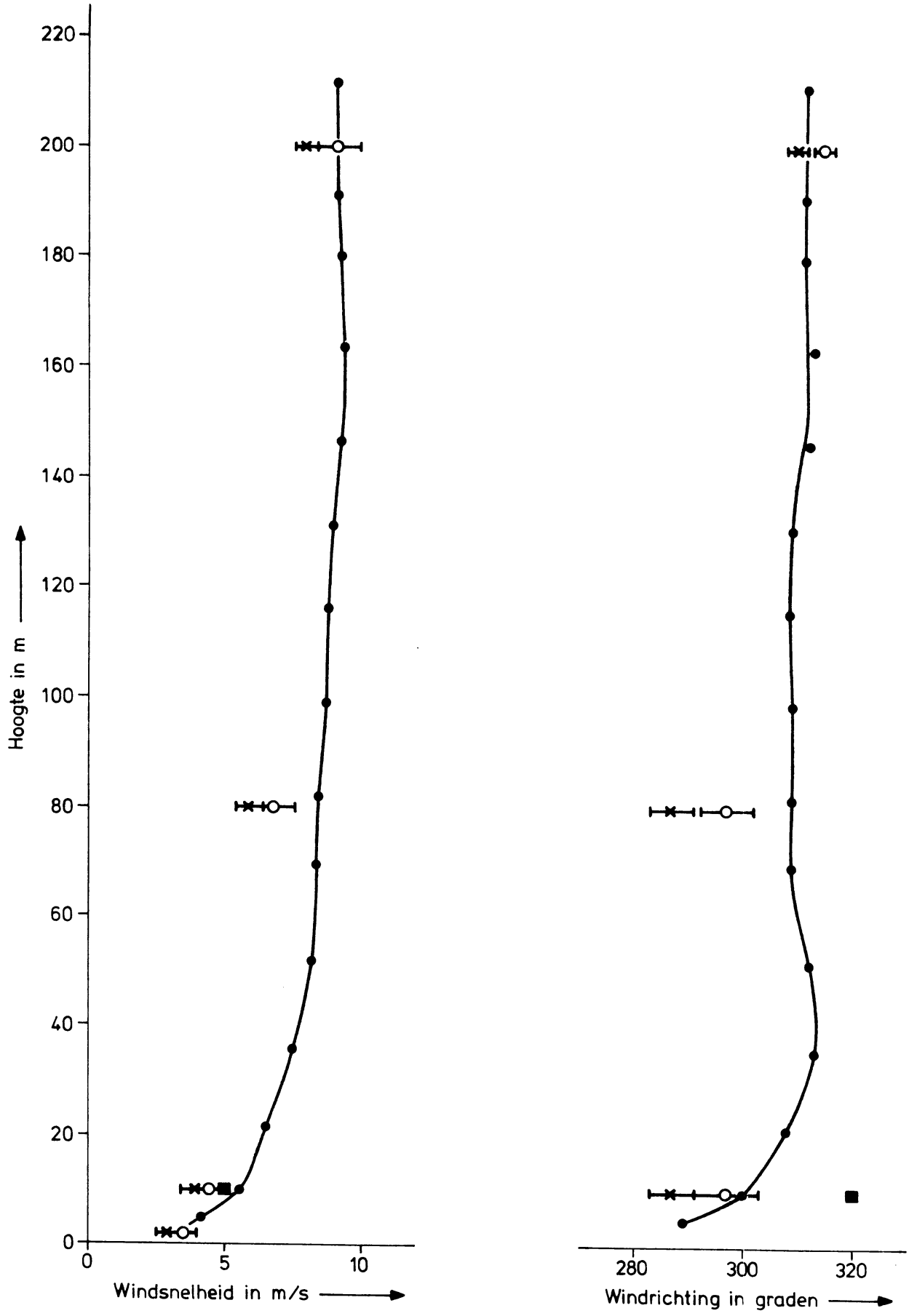

Fig. 3 Windsnelheid en windrichting gemeten tijdens een daling op 16-4-1975 om 06.20 GMT (touch-down tijd).

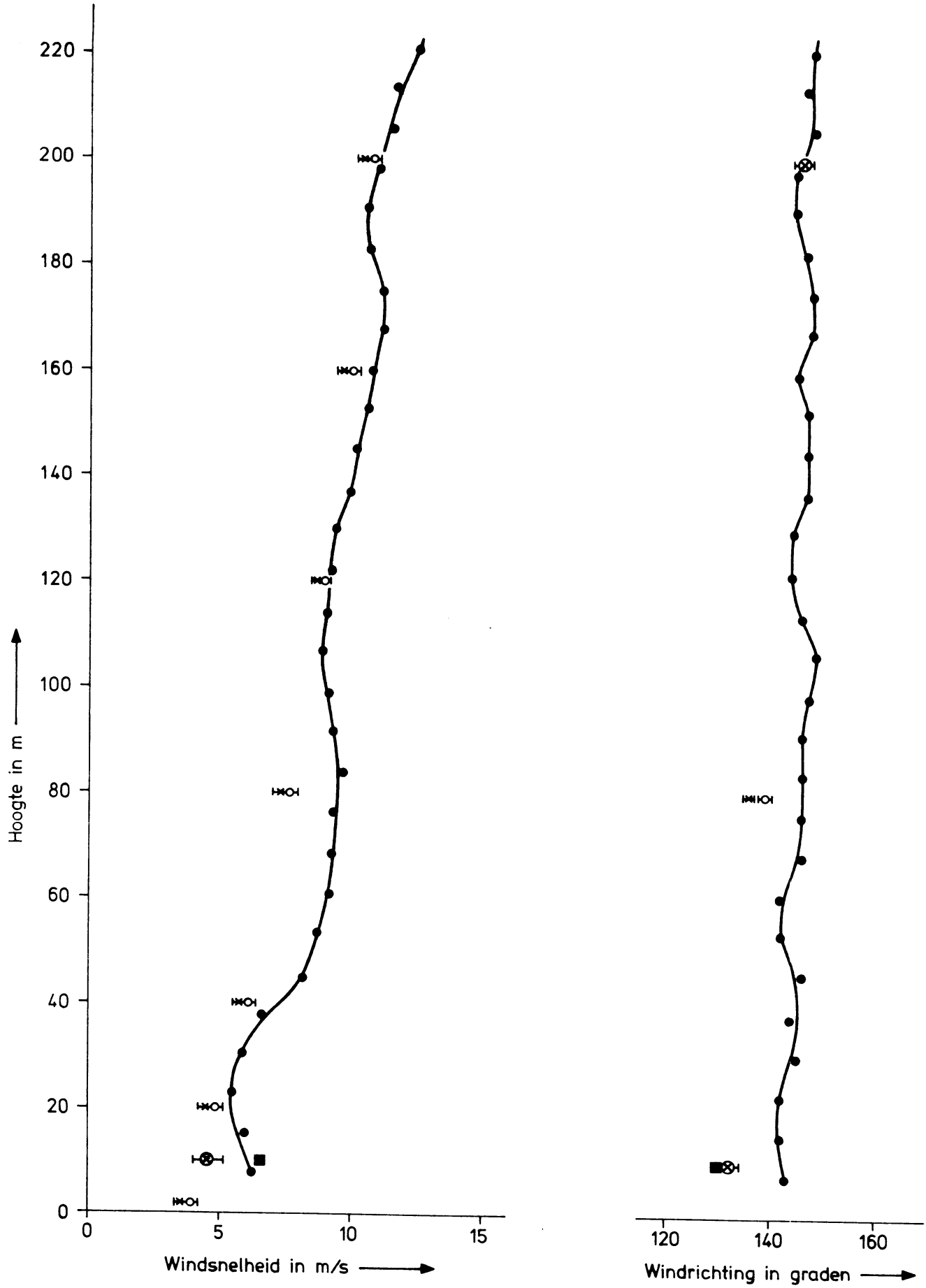

Fig. 4 Windsnelheid en windrichting gemeten tijdens een daling op 17-4-1975 om 18.00 GMT (touch-down tijd).

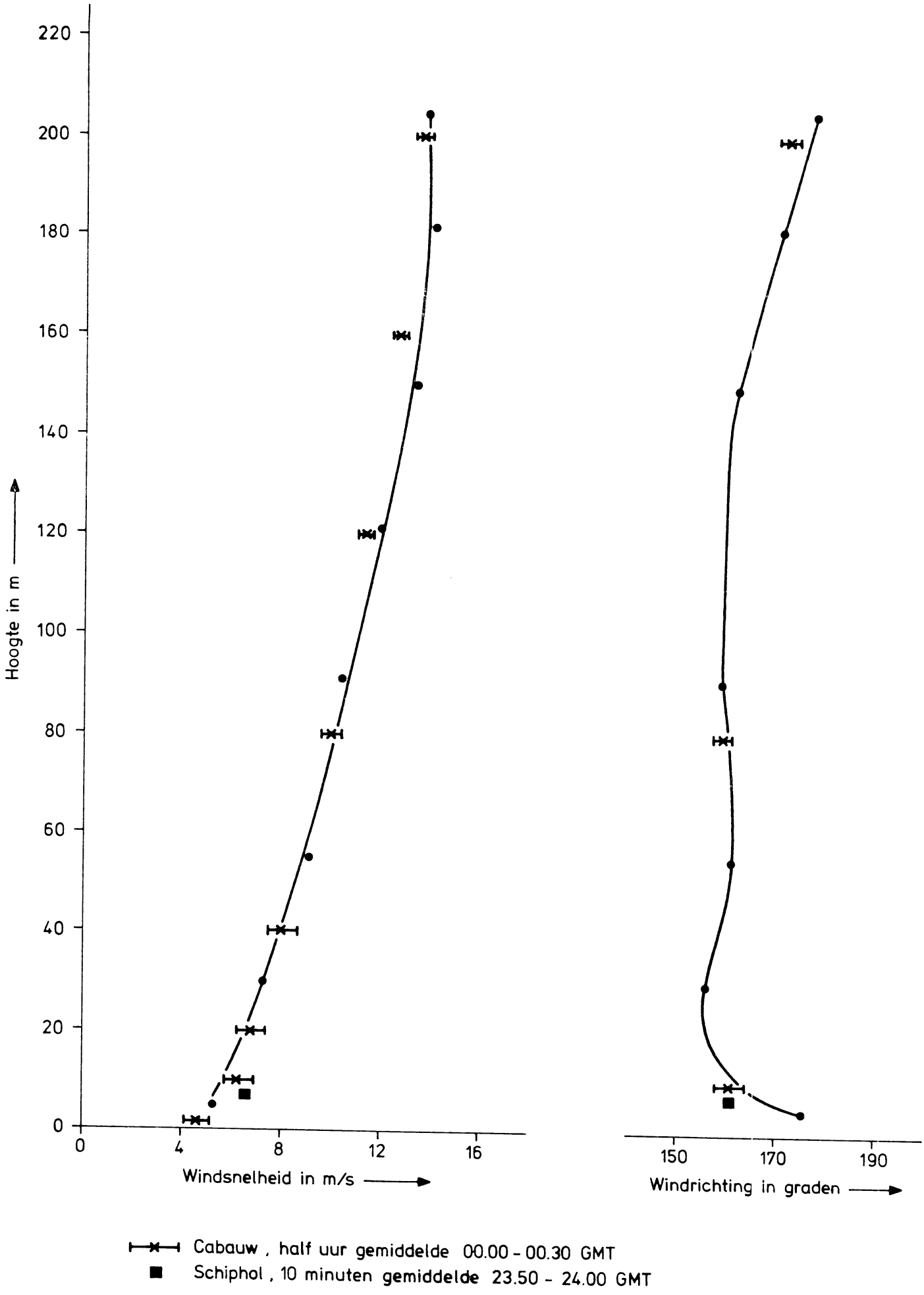

Fig. 5 Windsnelheid en windrichting gemeten tijdens een daling op 24-9-1974 om 00.08 GMT (touch-down tijd).

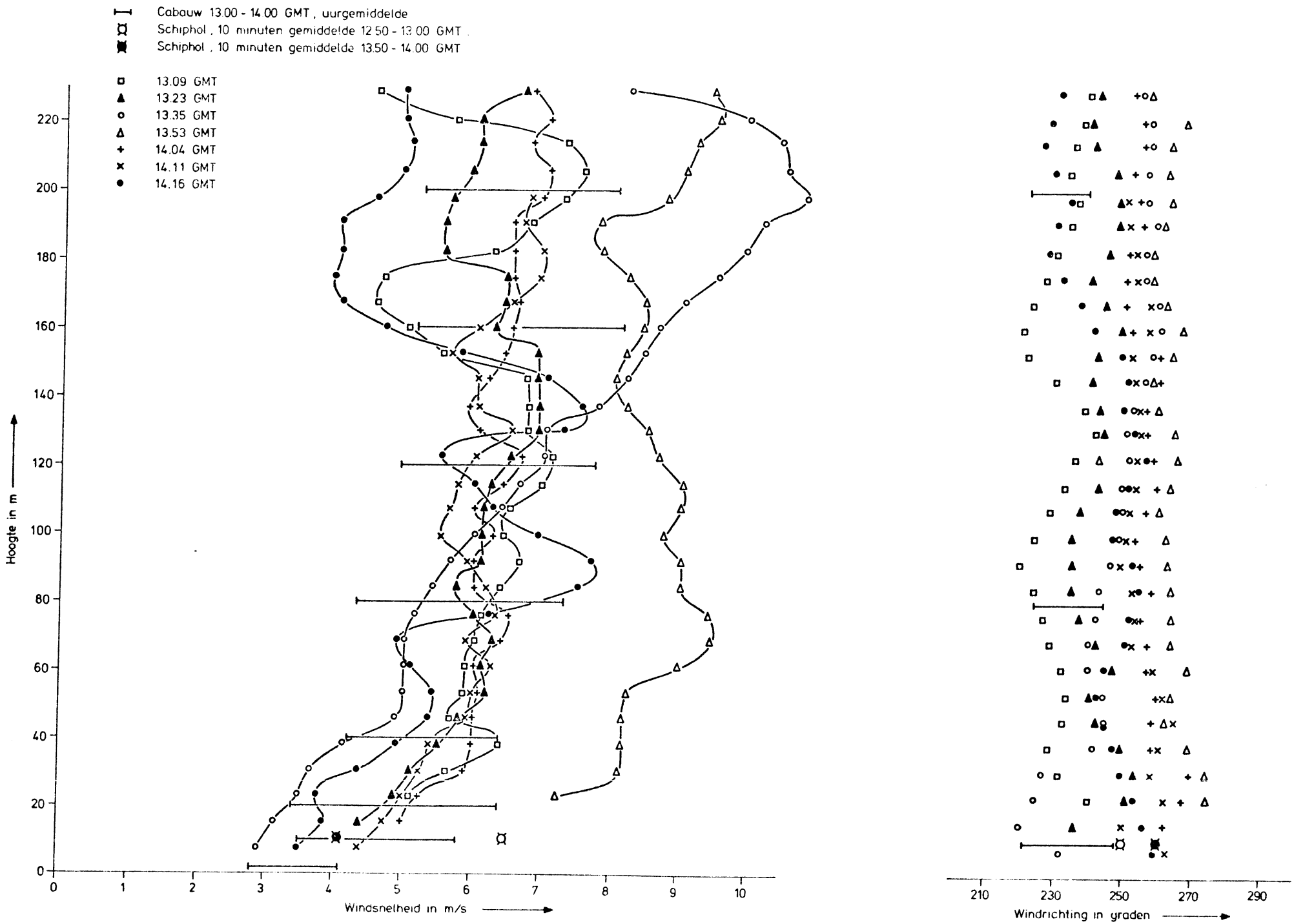

Fig. 6 Windsnelheid en windrichting gemeten tijdens zeven achtereenvolgende landingen op 15-4-1975.

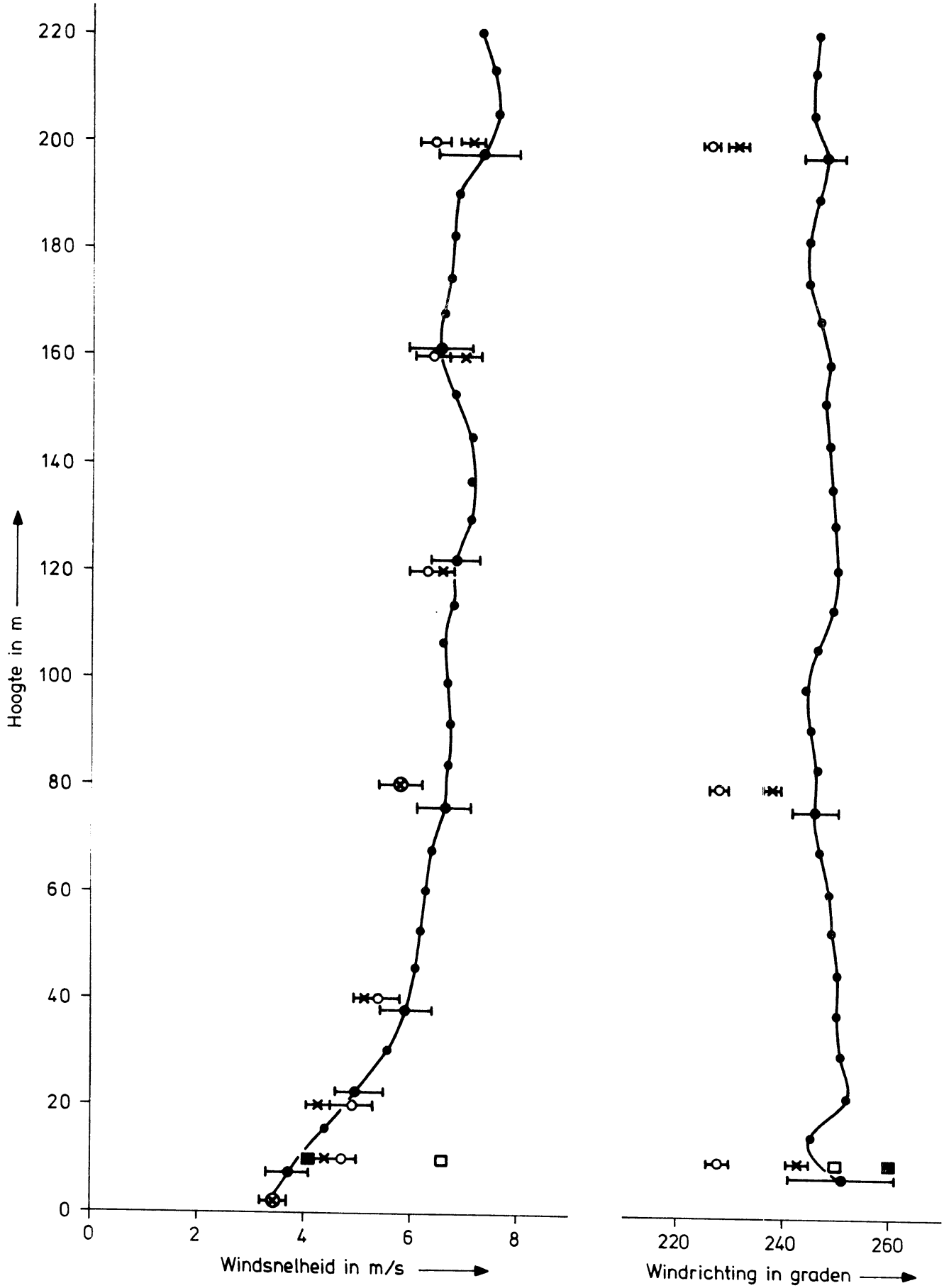

Fig. 7 Gemiddelde windsnelheid en windrichting verkregen uit de zeven profielen van Fig. 6.

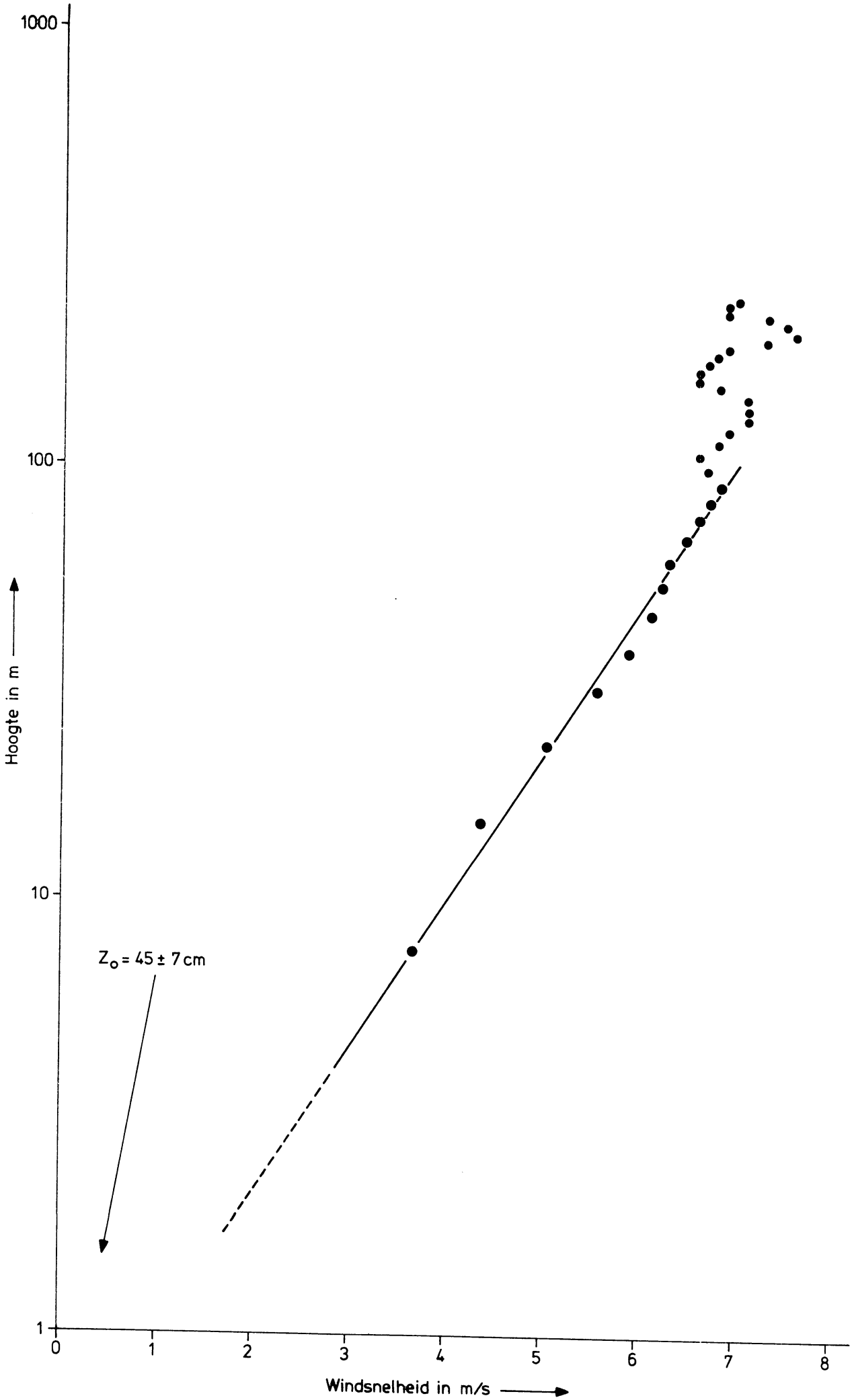

Fig. 8 Gemiddelde windsnelheid verkregen uit de zeven profielen van Fig. 6 uitgezet tegen de logaritme van de hoogte.

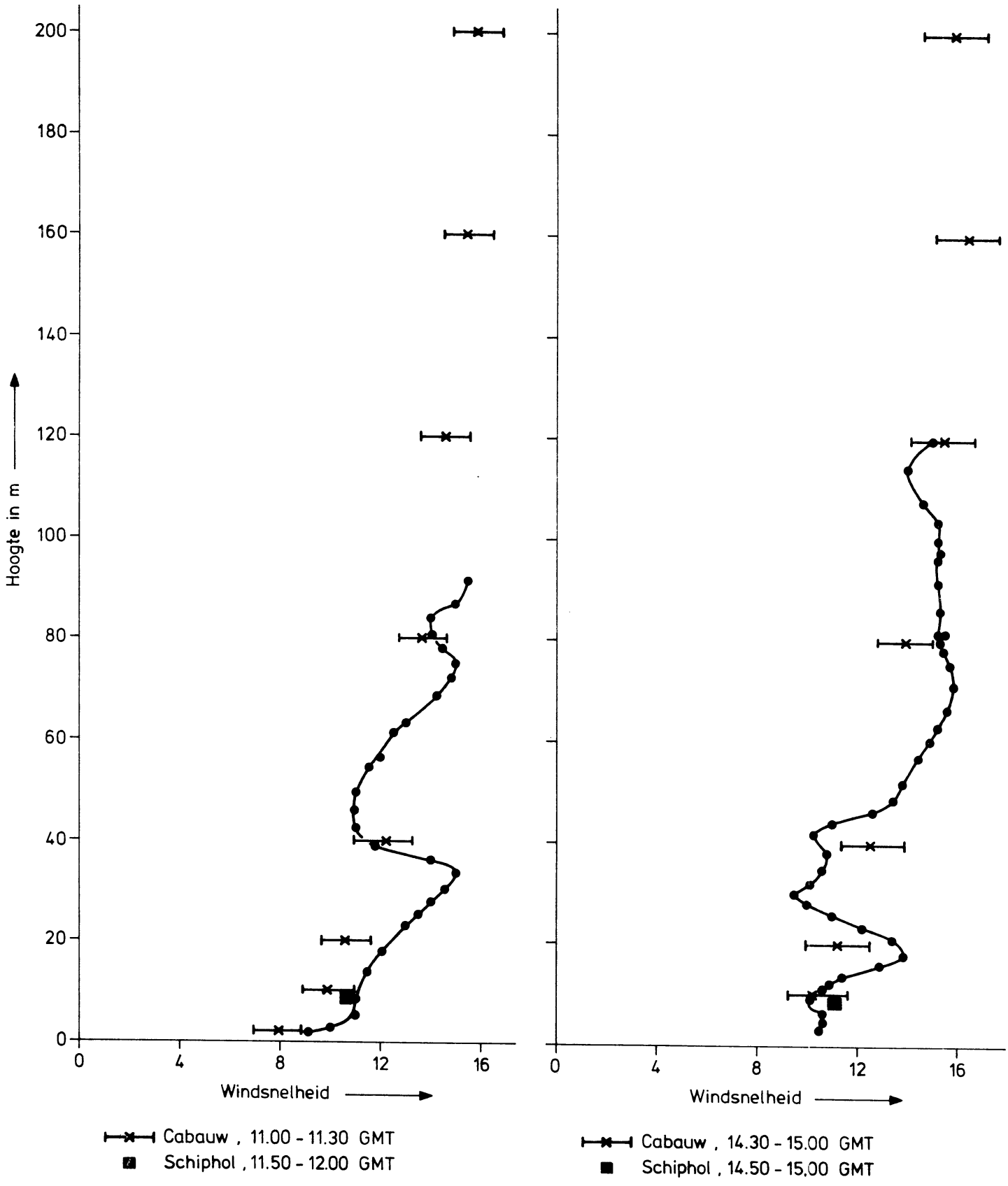

Fig. 9 Windsnelheid gemeten tijdens dalingen op 23-9-1974 om 11.27 GMT (linker profiel) en op 27-10-1974 om 15.00 GMT (rechter profiel).

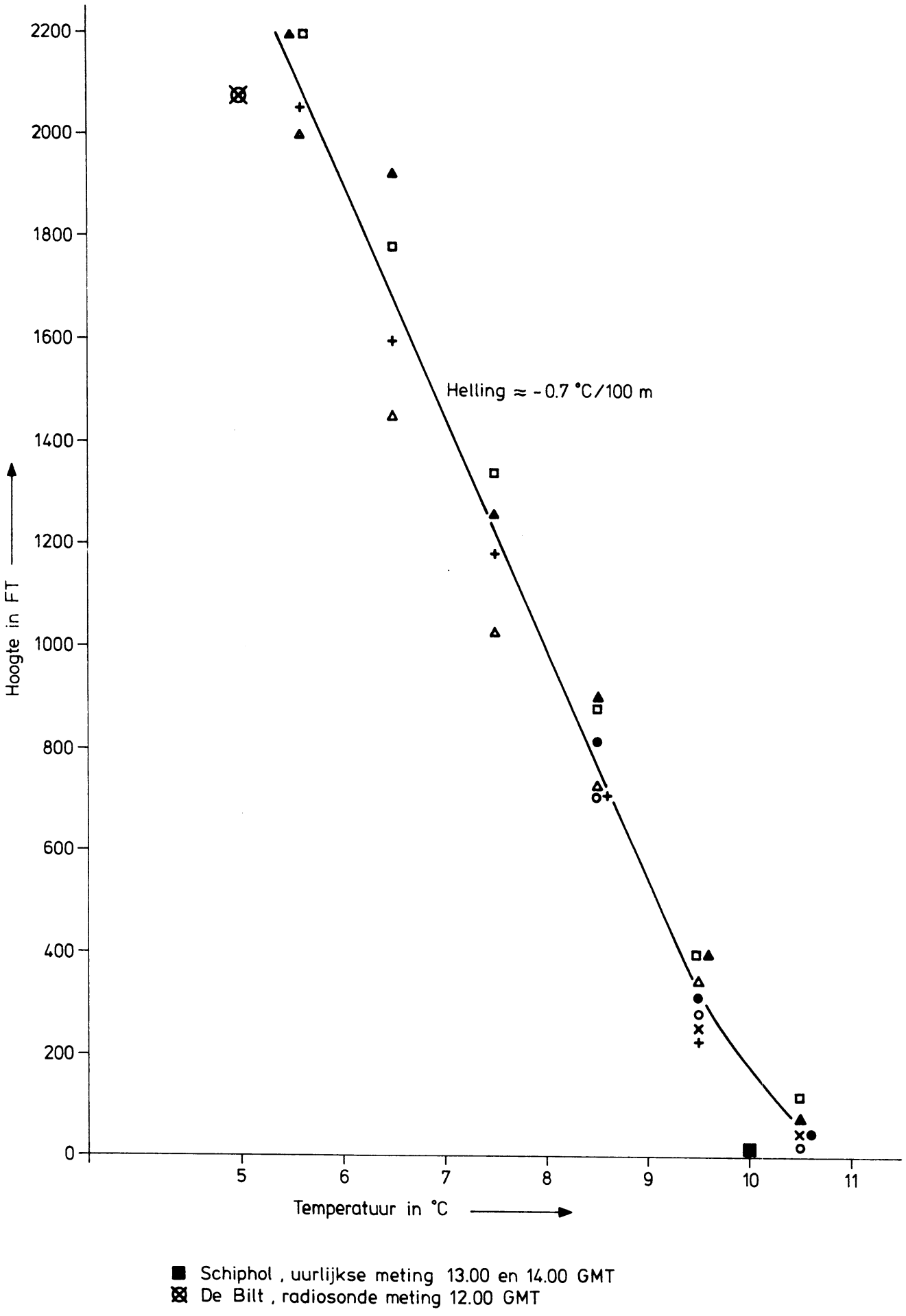

Fig. 10 Temperaturen gemeten tijdens de zeven achtereenvolgende dalingen op 15-4-1975. N.B. De hoogteschaal is in voeten.

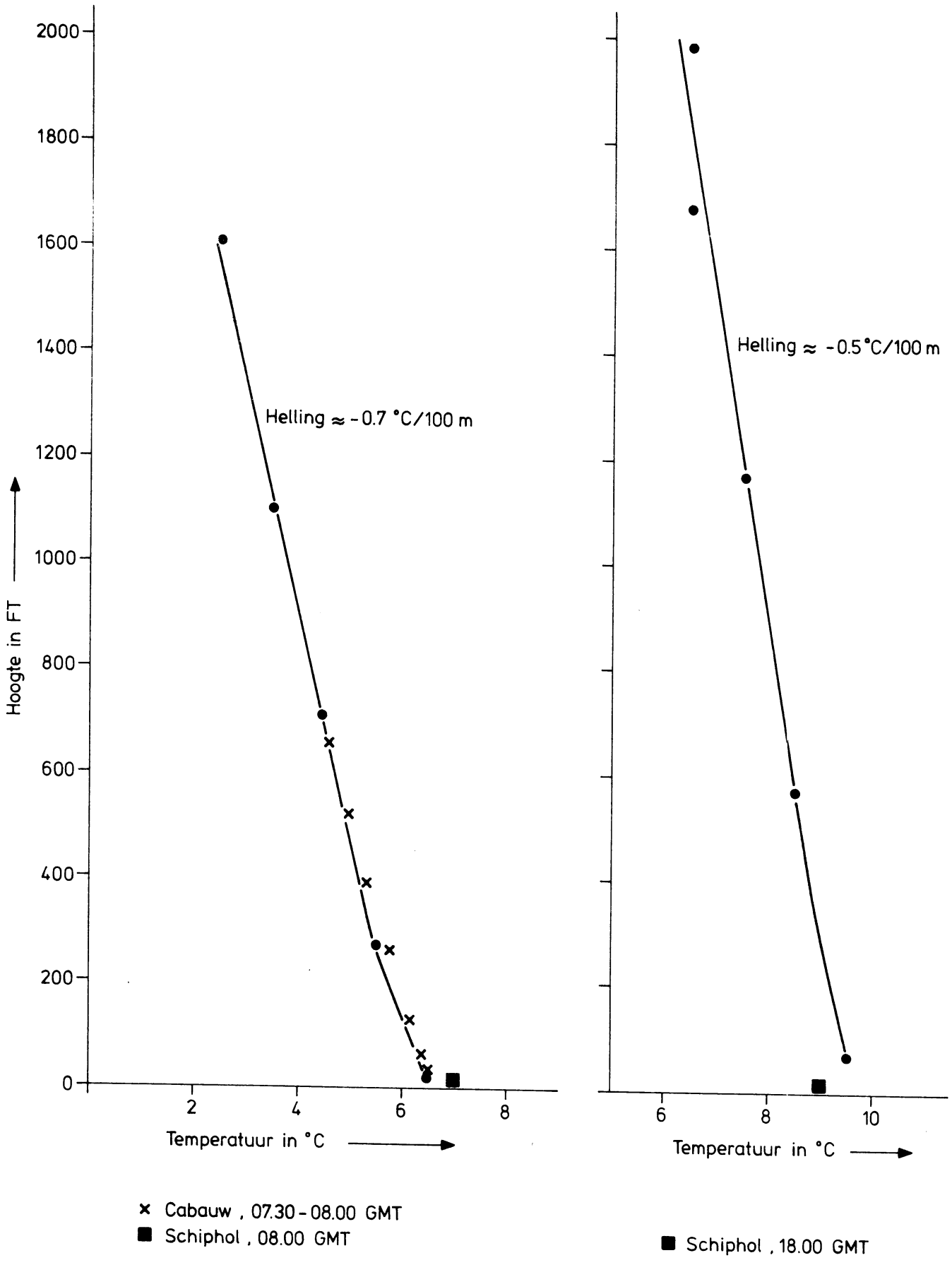

Fig. 11 Temperaturen gemeten tijdens dalingen op 16-4-1975 om 07.52 GMT (linker profiel) en op 17-4-1975 om 18.00 GMT (rechter profiel). N.B. De hoogteschaal is in voeten.